VANCOUVER PROSTATE CENTRE
A UBC & VGH Centre of Excellence

Addressing the Problem of Drug Resistance. Application of Network Theory for Identification of Novel Drug Targets

Artem Cherkasov
UBC

June. 26, 2014

The problem of resistance

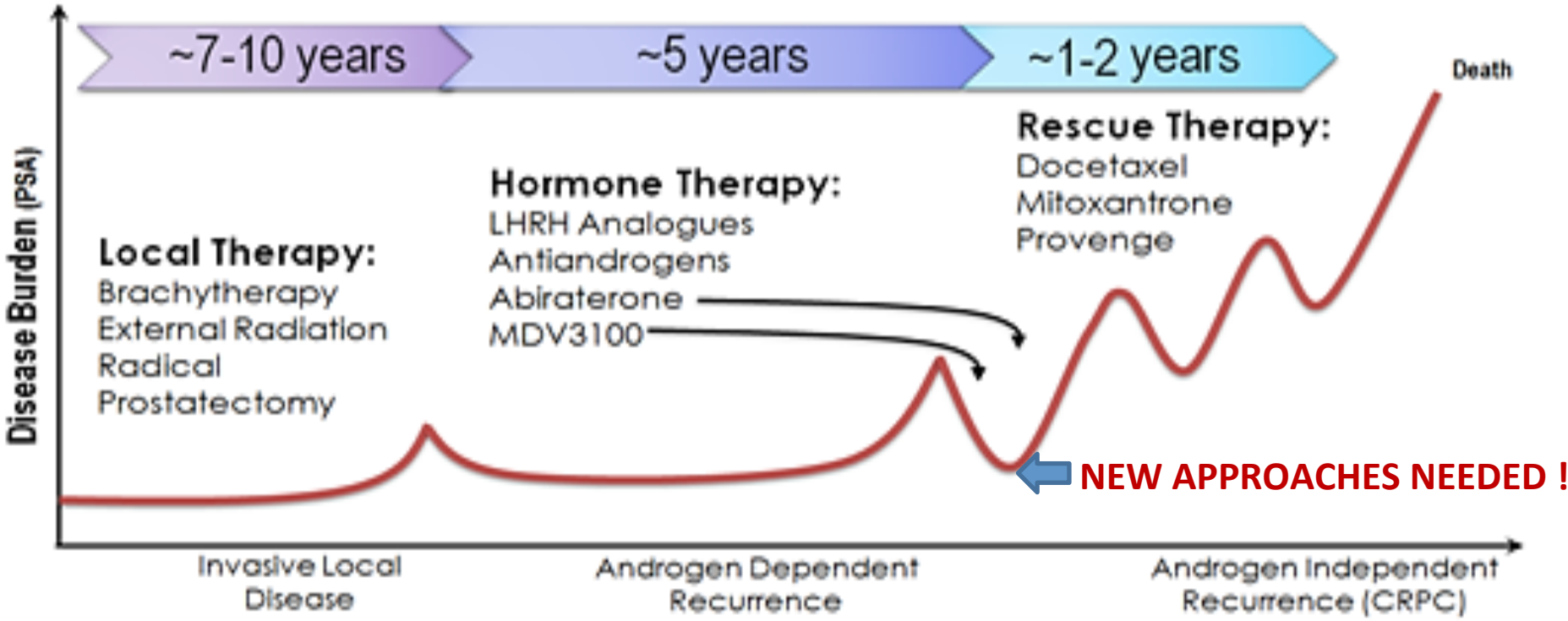

Protein interaction networks – Targets Source

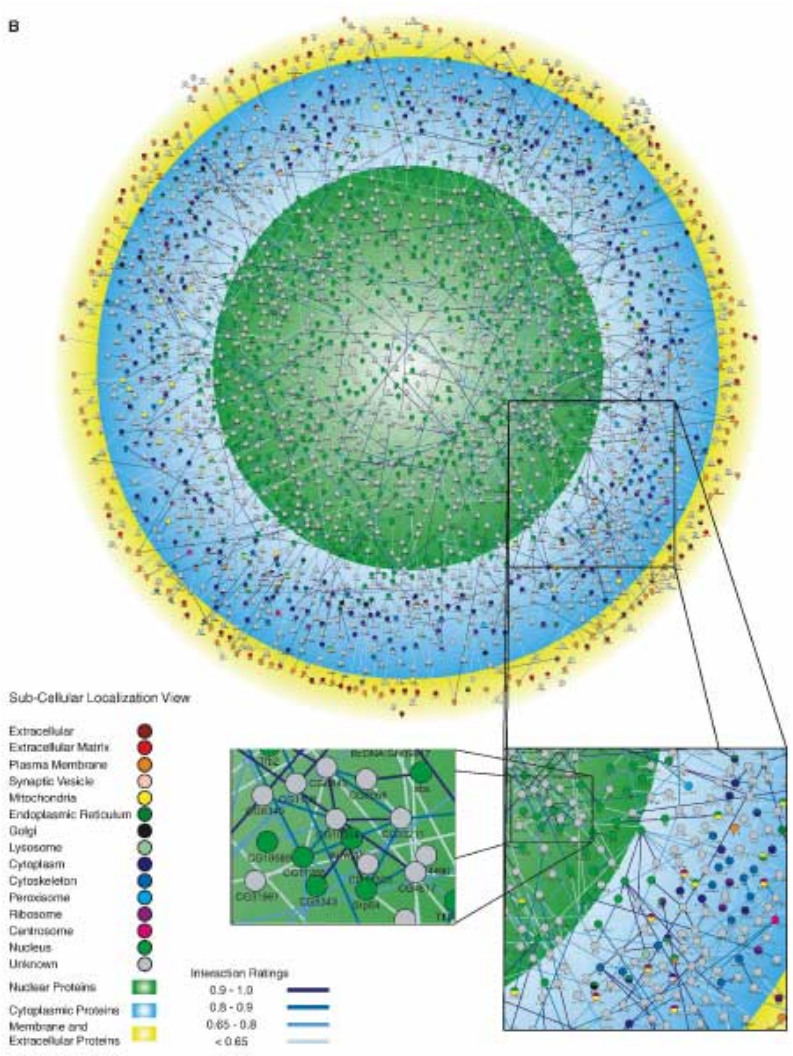

The web of human sexual contacts (Liljeros et al., Nature, 411 (2001) 907.

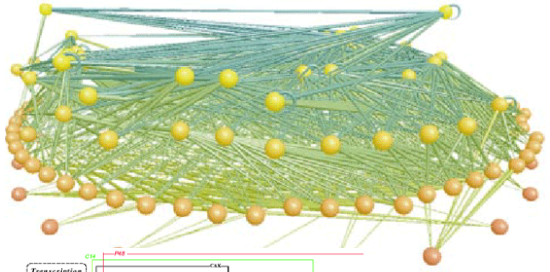

The Food Network

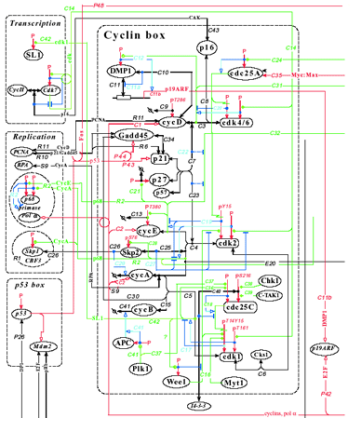

Neurons connections

Metabolic networks

Complex networks are scale-free

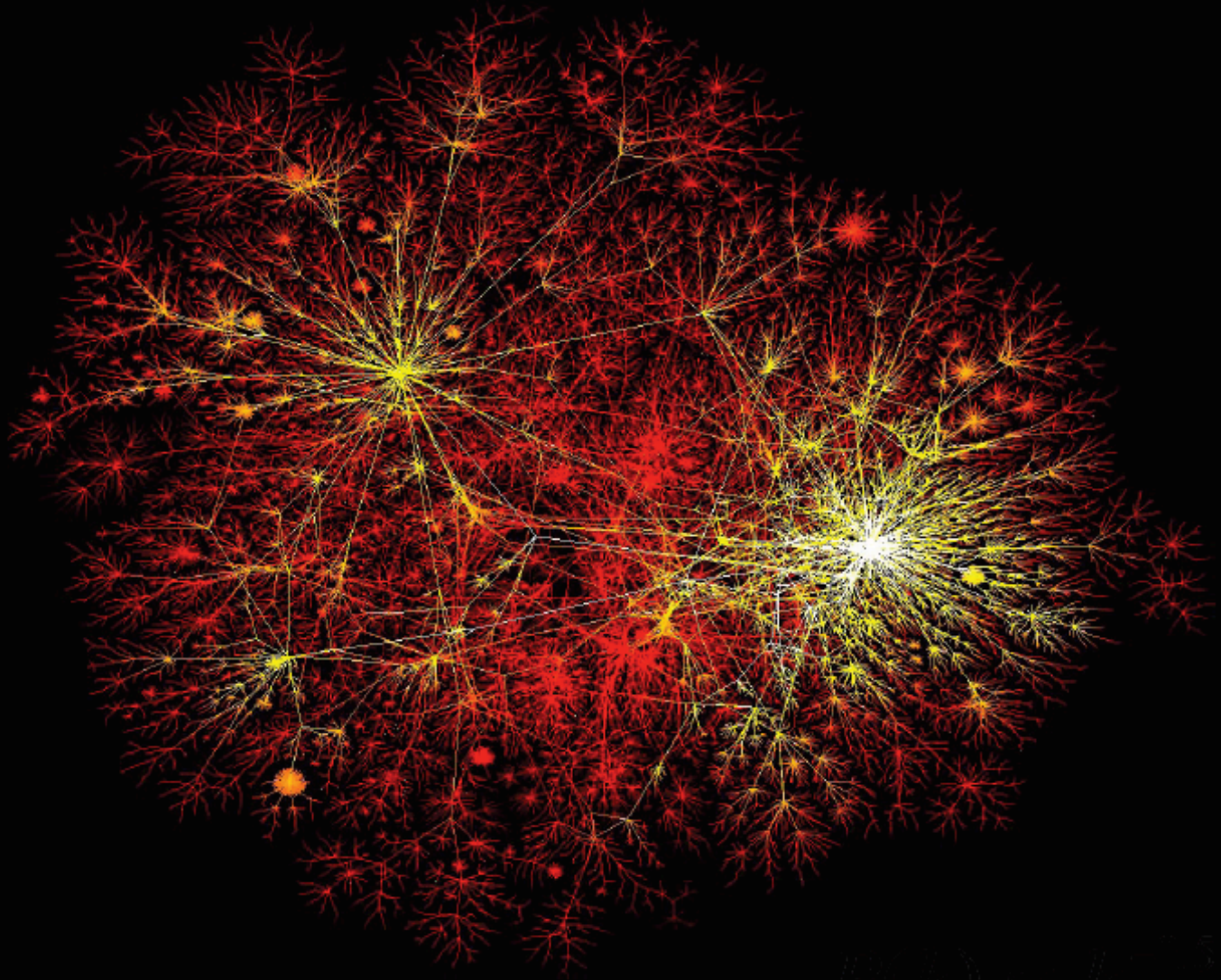

$$P(k) \sim k^{-\gamma}\phi(k/\xi)$$

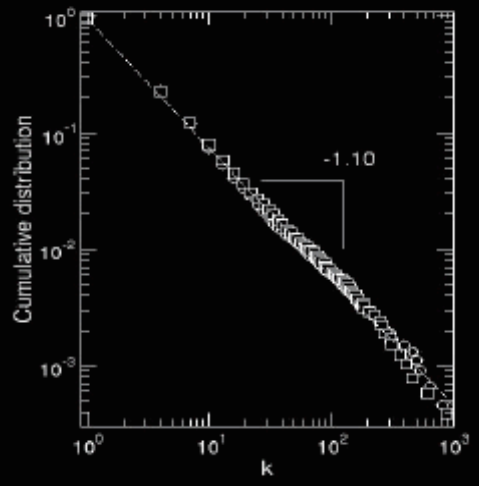

Barabási, Albert-László (2004). *Linked How Everything is Connected to Everything Else*

MRSA Proteins Interactions Network, 13,219 interactions, 608 proteins

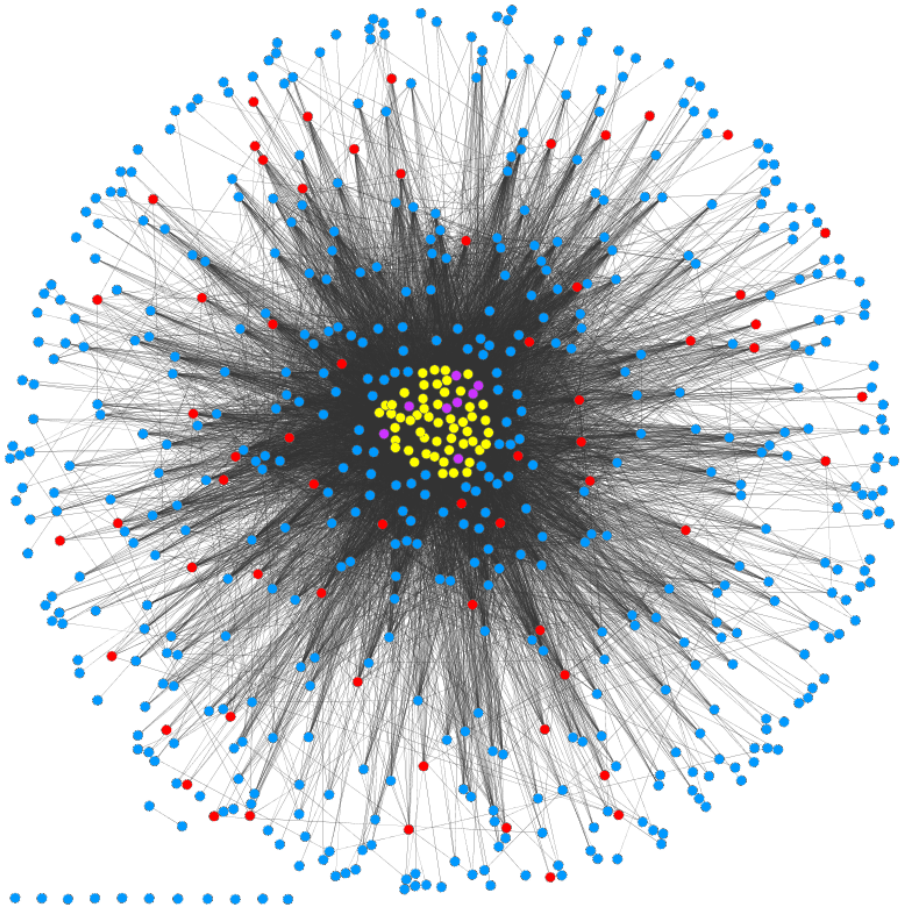

2D representation of the MS-MS derived MRSA PIN. Hub proteins are marked in yellow

The conventional antimicrobial targets are marked in red and they are NON-hubs!

A. Cherkasov et al, Prot Research 2011

Results: MRSA PIN analysis

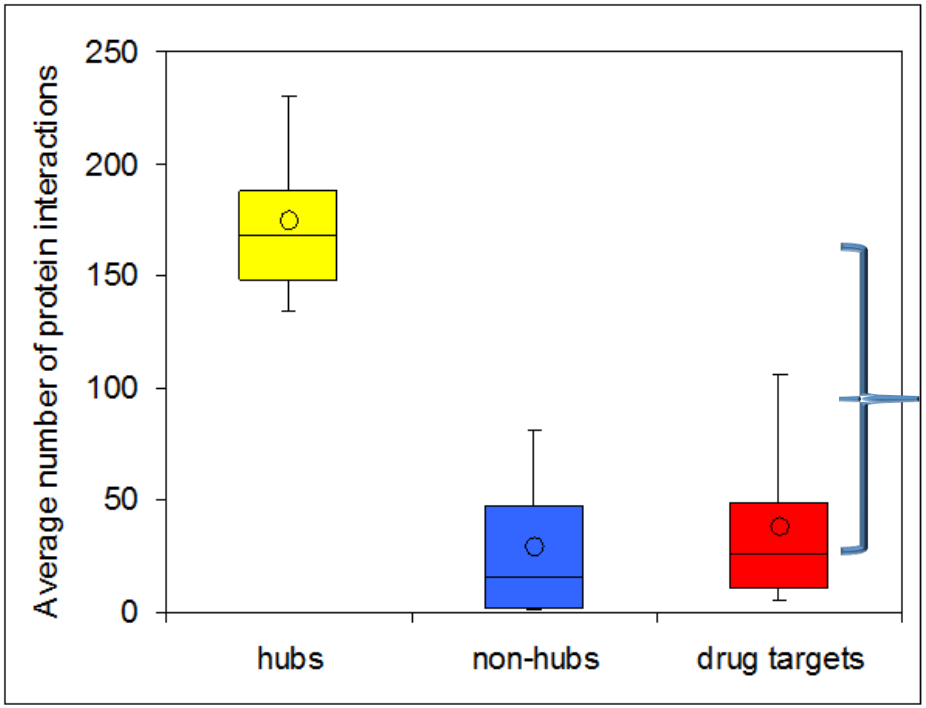

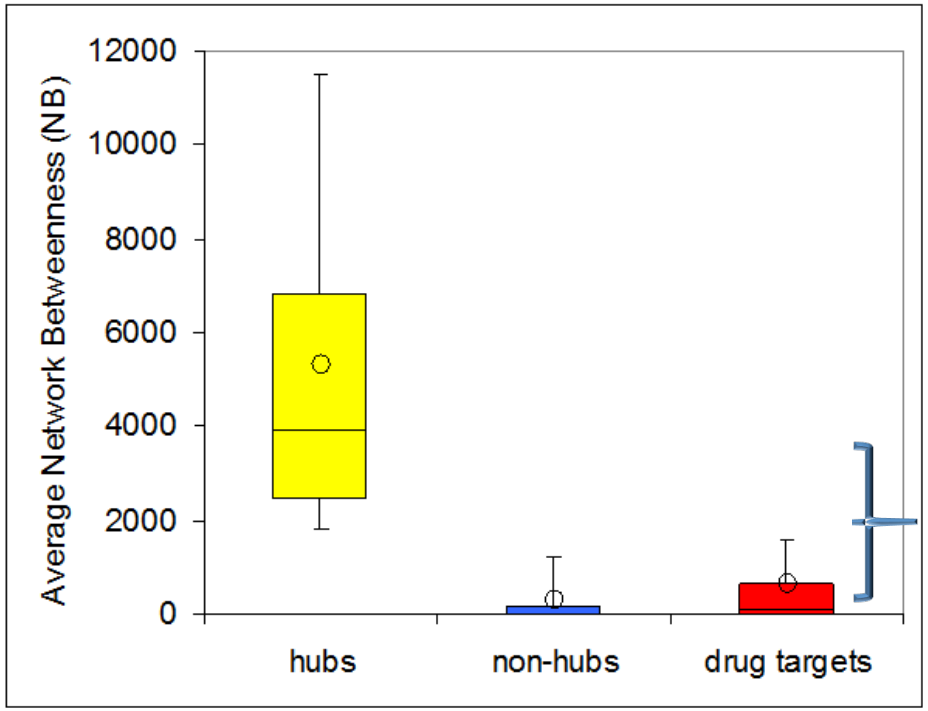

Average number of protein interactions among drug targets, hubs and non-hubs (left panel). Network Betweenness (NB) values for drug targets, hubs and non-hubs (right panel).

The conventional antimicrobial targets are NOT hubs!

WHY HUBS COULD BE BETTER TARGETS?

- MOST ESSENTIAL

- LESS ADAPTIVE (LOWER RATES OF MUTATION, SLOWER EVOLVING HOUSE-KEEPING GENES)

WHY HUBS COULD BE BAD TARGETS?

- MOST CONSERVED

- HOUSE-KEEPING PROTEINS WITH ORTHOLOGUES (CANCER) AND PARALOGUES (ANTIBIOTICS)

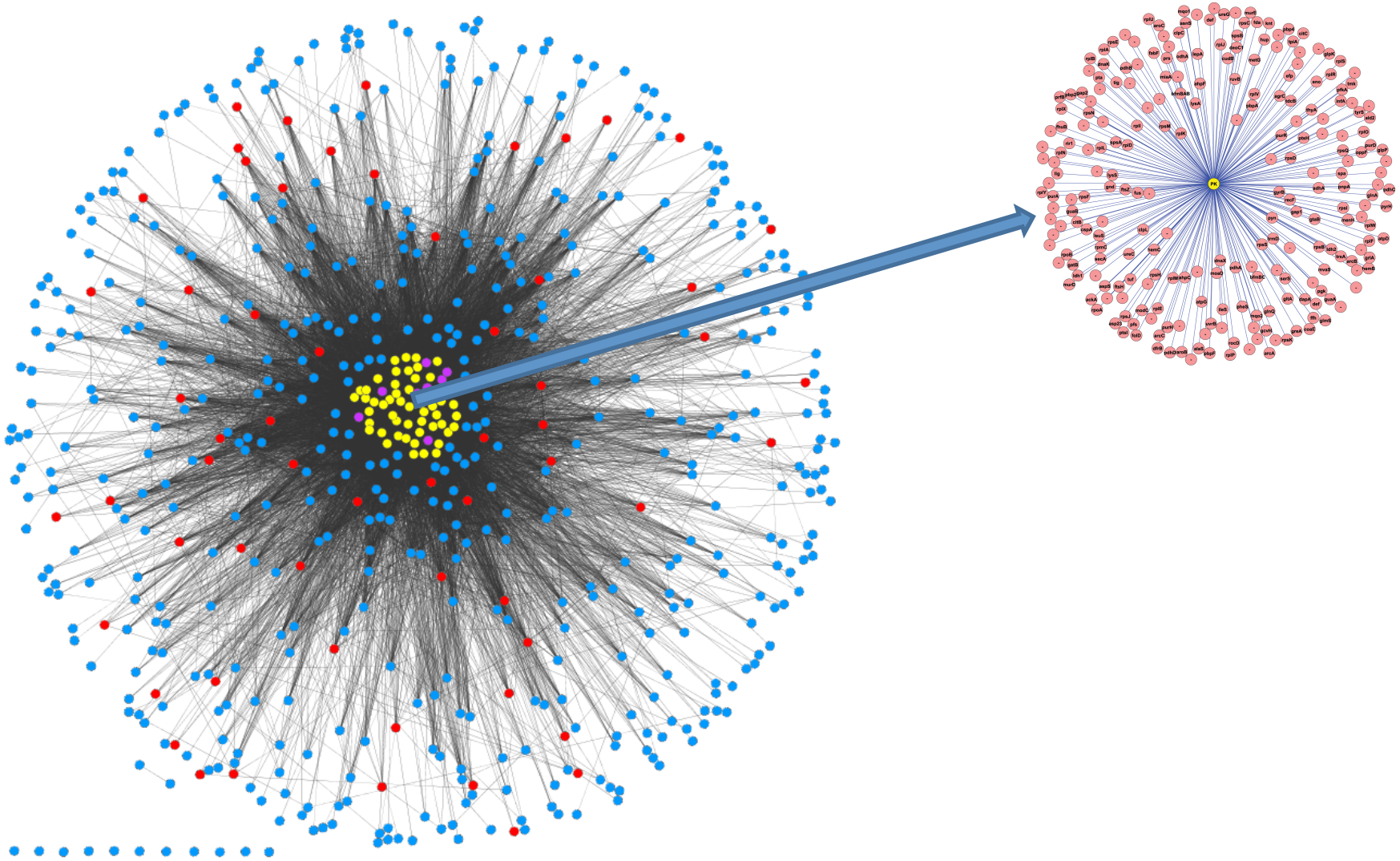

A. Cherkasov et al, *Prot Research* 2011

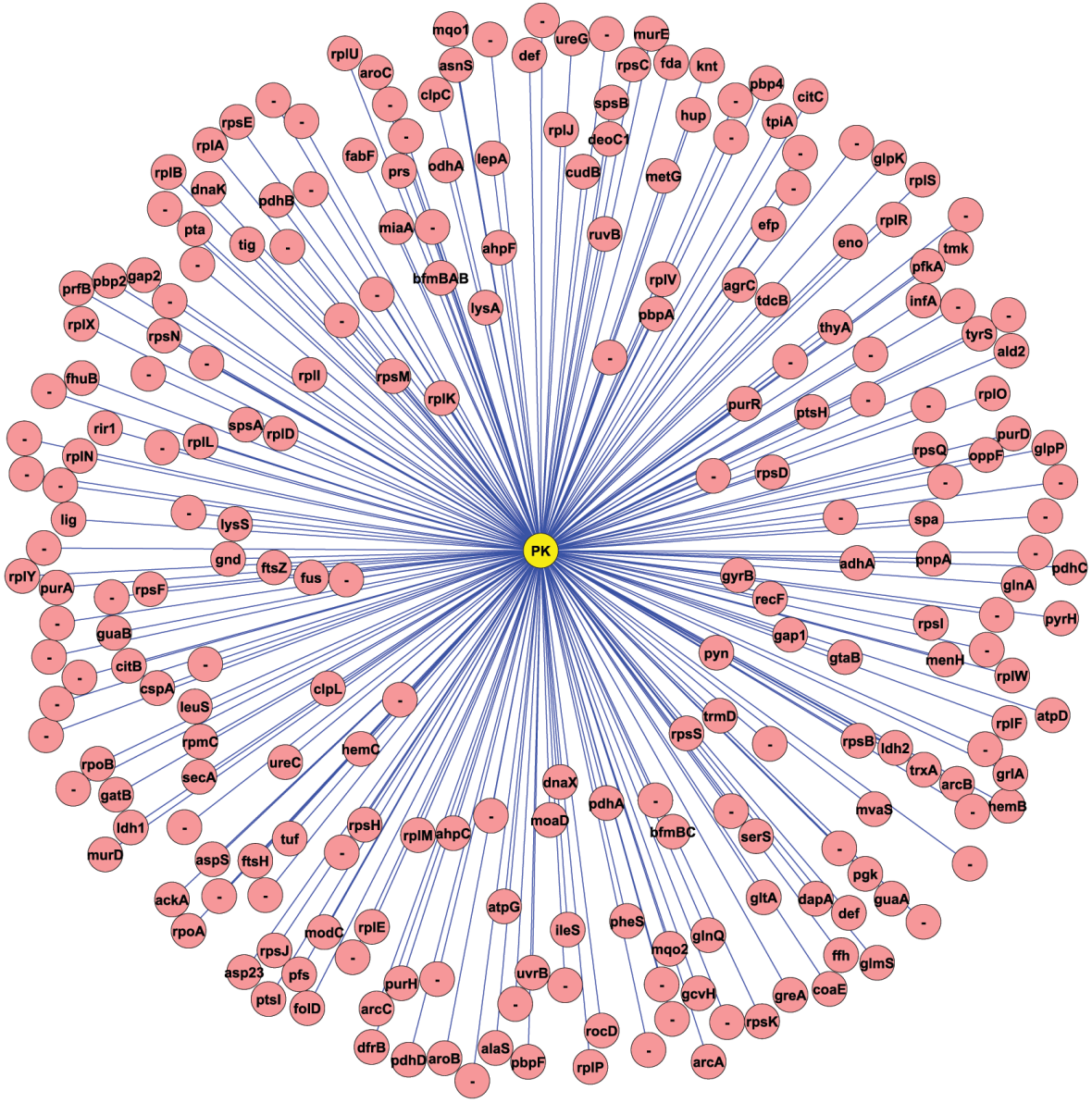

2D representation of Pyurvate Kinase in the context of its protein-protein interactions.

THE UNIVERSITY OF BRITISH COLUMBIA

Pyruvate Kinase

- Pyruvate kinase (PK) was identified as a highly connected hub protein in MRSA.
  - Essential for S. aureus viability.
  - Pyruvate is used in a number of biosynthetic pathways, placing PK at a pivotal metabolic intersection.

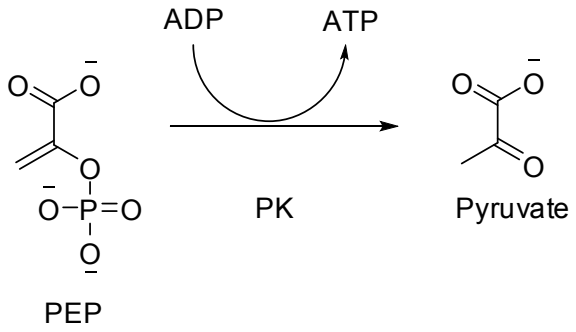

MRSA Pyruvate Kinase (PK) might be a good HUB target,

BUT

highly similar to human PKs

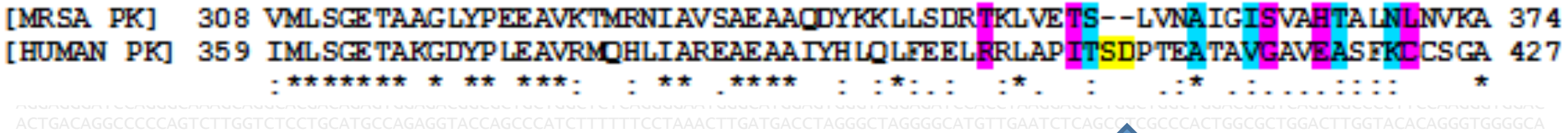

IN(sertions) DEL(etions) = INDELs

```
[MRSA PK]   308 VMLSGETAAGLYPEEAVKTMRNIAVSAEAAQDYKKLLSDRTKLVETS--LVNAIGISVAHTALNLNVKA 374
[HUMAN PK]  359 IMLSGETAKGDYPLEAVRMQHLIAREAEAAIYHLQLFEELRRLAPITSDPTEATAVGAVEASFKCCSGA 427
                :******* * ** ***:   : ** .****   : :*:.:   :*.   :    .:* .:.....::::     *
```

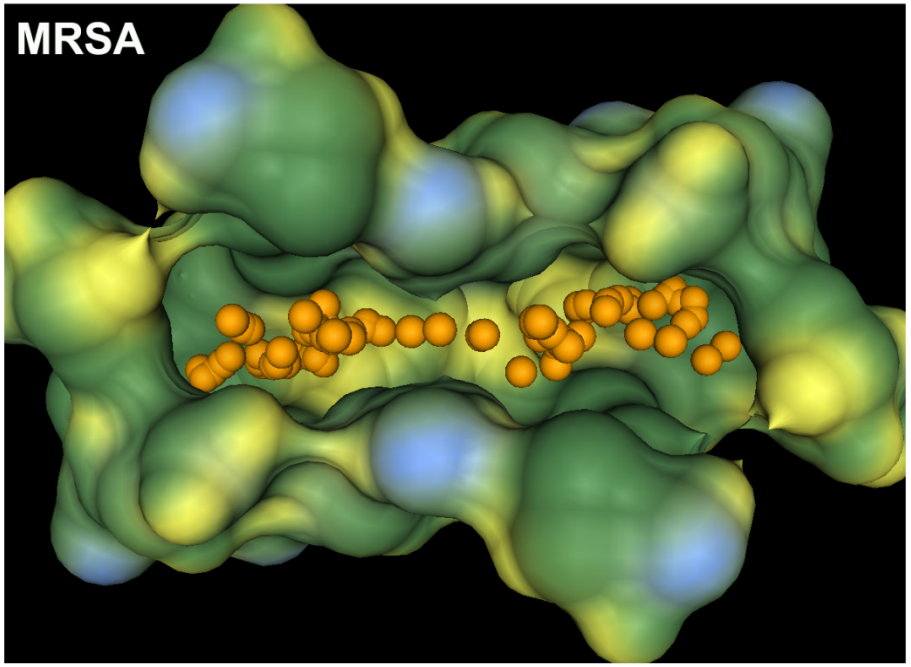

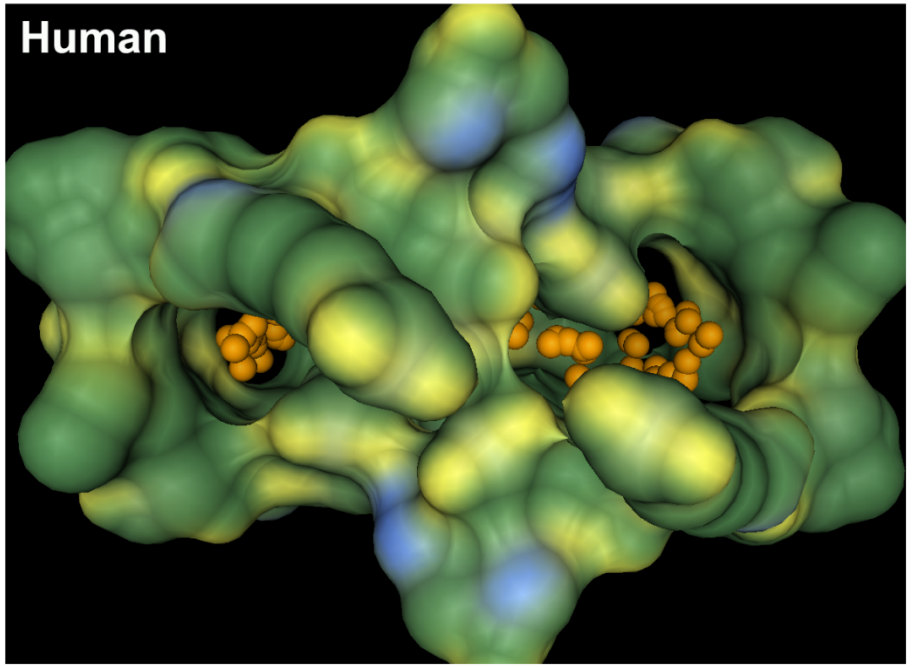

Structural model of the interface-binding site for MRSA and human PK. Orange spheres show the interface cavity in MRSA and human.

The MRSA PK model shows an assessable binding pocket located at the interface of two PK monomers. Whereas, the pocket in human PK is partially closed by five amino acid residues (Glu418-B, Arg399-A, B and Arg400-A, B).

VIRTUAL SCREENING PIPELINE

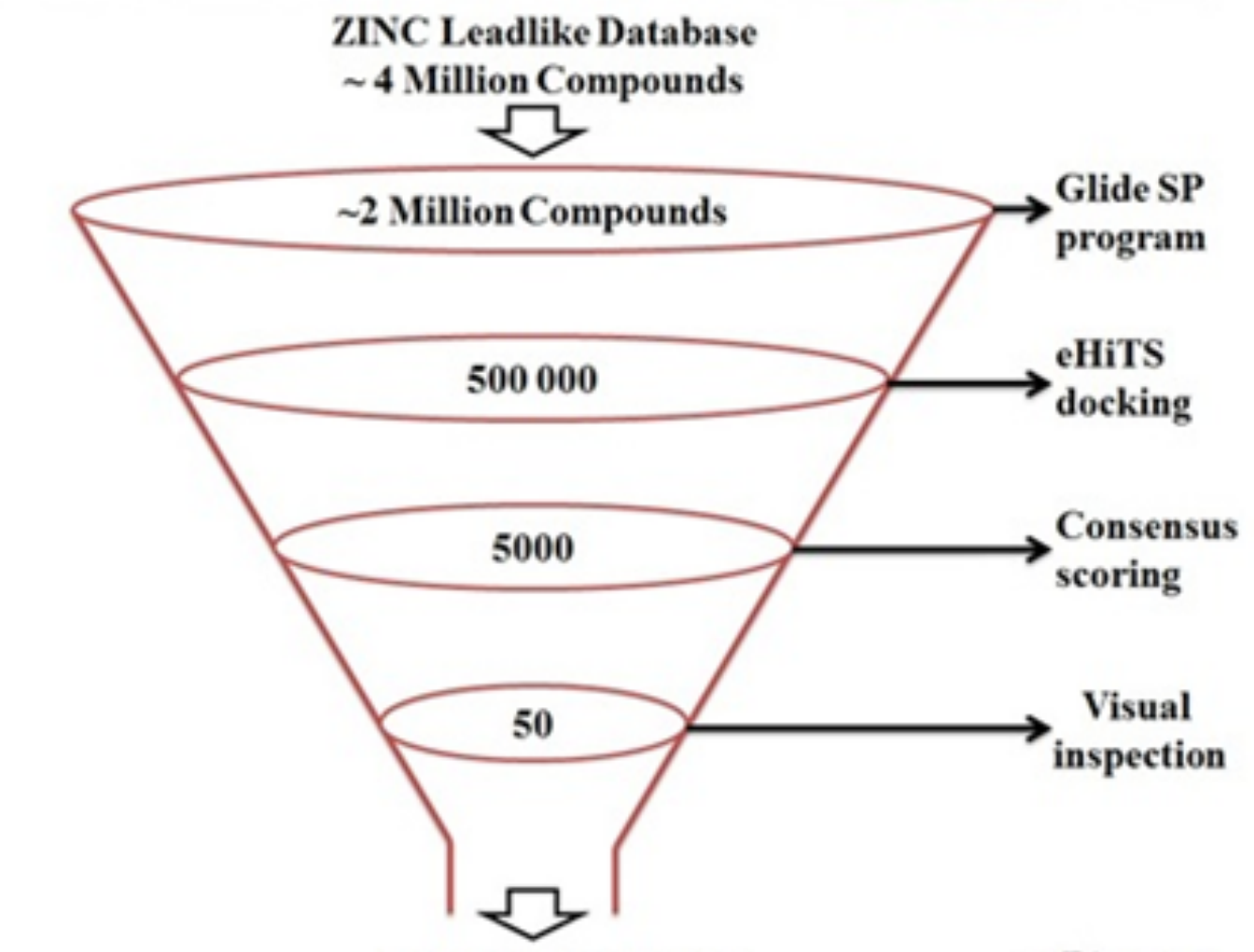

Can 'Bacterial-Metabolite-Likeness' Model Improve Odds of 'in Silico' Antibiotic Discovery?

Artem Cherkasov*

Division of Infectious Diseases, Faculty of Medicine, University of British Columbia, 2733 Heather Street, Vancouver, British Columbia V5Z 3J5, Canada

Received November 1, 2005

'Inductive' QSAR descriptors have been used to develop the series of QSAR models enabling 'in silico' distinguishing between antimicrobial compounds, conventional drugs, and druglike substances. The constructed neural network-based models operating by 30 'inductive' parameters have been validated on an extensive set of 2686 chemical structures and resulted in up to 97% accurate separation of the three types of molecular activities. The demonstrated ability of 'inductive' parameters to adequately capture molecular features determining 'antibiotic-like' and 'druglike' potentials have been further utilized to construct a model of 'Bacterial-Metabolite-Likeness' (BML). The same 'inductive' descriptors have been used to train a neural network that could very accurately recognize substances involved into bacterial metabolism (that have been experimentally identified). When the developed model has been applied to the mixed set of antimicrobials, drugs, and druglike chemicals (not used for training the BML model), it exhibited a 2−5-fold recognition preference toward antimicrobial compounds compared to general drugs and an 18- to 45-fold preference when compared to a druglike substance (depending on the model stringency). These results illustrate immanent similarity between conventional antimicrobials and native bacterial metabolites and suggest that the developed BML model can be an effective classification tool for 'in silico' antibiotic studies.

INTRODUCTION

In the series of our previous works we reported the development of 3D-sensitive QSAR descriptors called 'inductive' and demonstrated their successful application in a number of molecular modeling studies including quantification of antibacterial activity of organic compounds[1] and cationic peptides,[1,2] computation of partial charges in small molecules[3] and proteins,[4] and in comparative docking analysis[4,5] as well as in 'in silico' lead discovery.[4,5] The detailed description of 'inductive' QSAR descriptors and their rationale can be found in the recent review.[1]

In summary, all 'inductive' QSAR parameters are related to atomic electronegativity (χ), covalent radii (R), and

$$\sigma^*_{j\rightarrow N-1} = \beta \sum_{i\neq j}^{N-1} \frac{(\chi_j^0 - \chi_i^0)R_j^2}{r_{j-i}^2}$$

$$\sigma^*_{C\rightarrow j} = \beta \sum_{i\subset C, i\neq j}^{n} \frac{(\chi_i^0 - \chi_j^0)R_i^2}{r_{i-j}^2} \quad (2)$$

$$\chi_{N-1\rightarrow j}^0 = \frac{\sum_{i\neq j}^{N-1} \frac{\chi_i^0(R_i^2 + R_j^2)}{r_{i-j}^2}}{\sum_{i\neq j}^{N-1} \frac{R_i^2 + R_j^2}{r_{i-j}^2}} \quad \chi_{N-1\rightarrow j}^0 = \frac{\sum_{i\neq j}^{N-1} \frac{\chi_i^0(R_i^2 + R_j^2)}{r_{i-j}^2}}{\sum_{i\neq j}^{N-1} \frac{R_i^2 + R_j^2}{r_{i-j}^2}} \quad (3)$$

DOCKING

50 cmps

4 hits

ID	structure	IC50 MRSA PK, μM	MIC MRSA μM	I	II	III	IV	V
IS-63	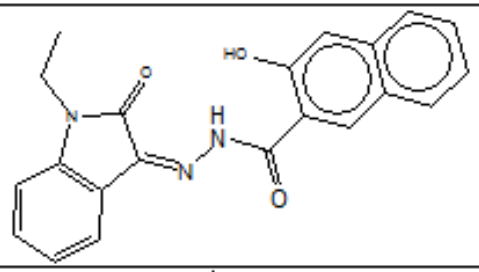	0.911	>500	83.9	15	1.3	13.5	22.2
IS-168	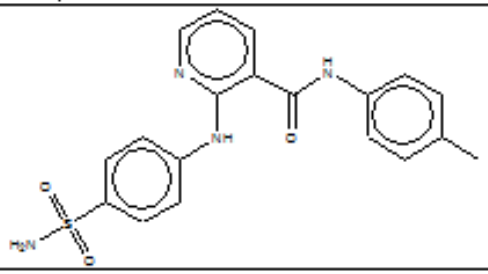			79.5	17.6	12.6	30.6	24.7
IS-53	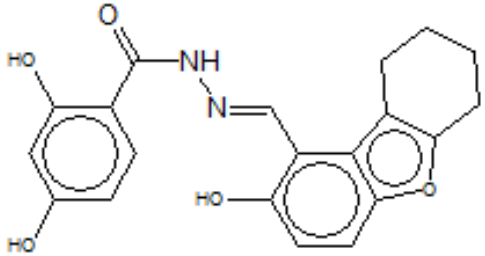			77.8	39.3	57.5	78.1	87.8
IS-165	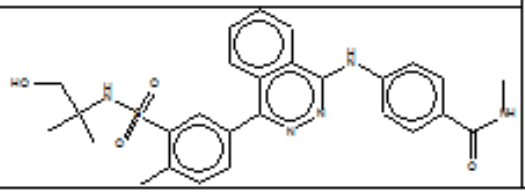			54.6	25.8	8.3	15.3	9.4

ID	structure	IC 50 MRSA PK, µM	MIC MRSA µM	I	II	III	IV	V
IS-63	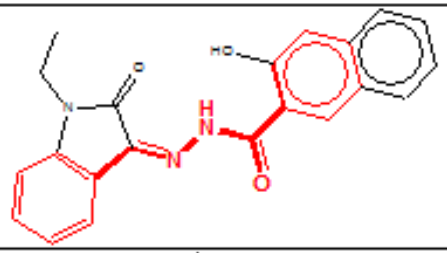	0.911	>500	83.9	15	1.3	13.5	22.2
IS-168	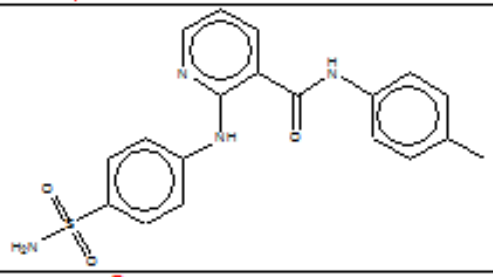			79.5	17.6	12.6	30.6	24.7
IS-53	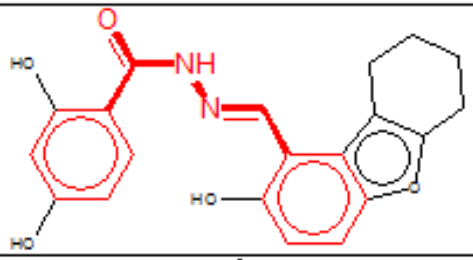			77.8	39.3	57.5	78.1	87.8
IS-165	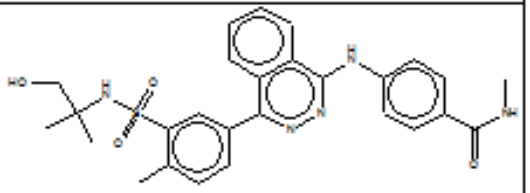			54.6	25.8	8.3	15.3	9.4

TOPOLOGICAL QUERRY

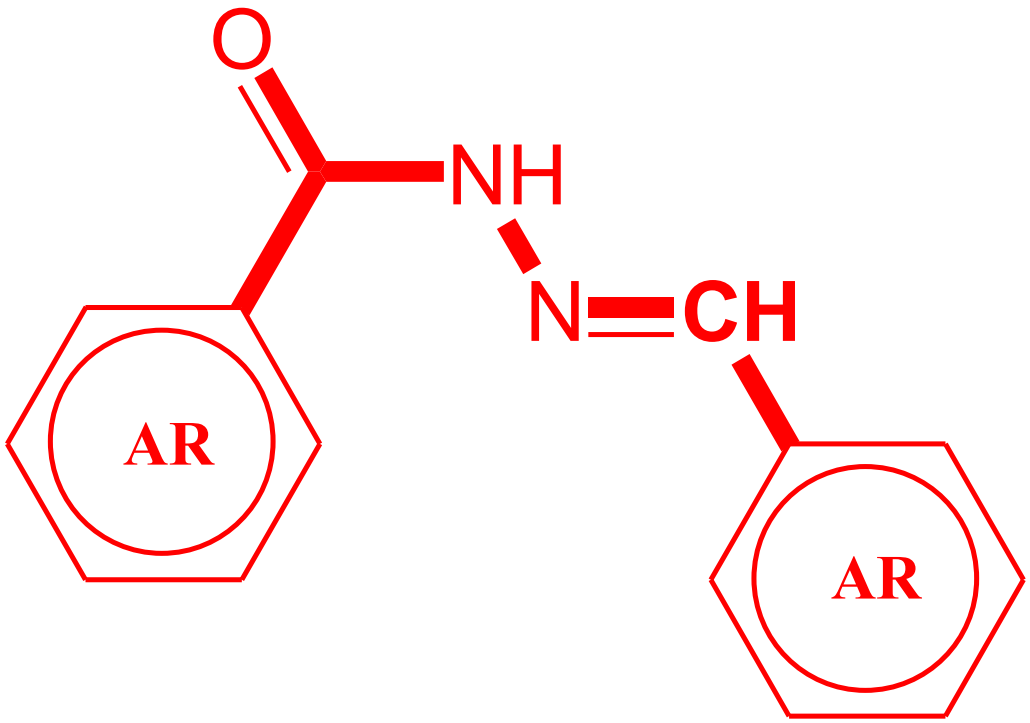

LIGAND-BASED SEARCH

50 cmps

6 hits

structure	IC50 MRSA PK, µM	MIC MRSA µM	I	II	III	IV	V	Tanimoto to IS-63
IS-130 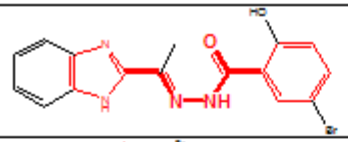	0.091	>500	98.5	-8.7	-11.9	-1.2	-2.1	0.63
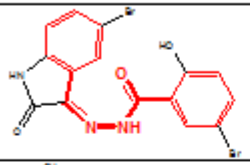			78.8	10.9	10.2	7.3	-4.7	0.72
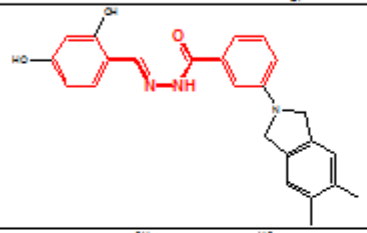			78.3	22.8	26.7	15.7	20.8	0.76
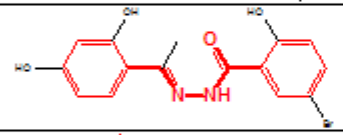			71.1	-1.7	2.2	9.8	0.9	0.60
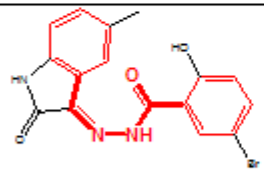			66.4	13.0	11.8	7.1	-1.0	0.76
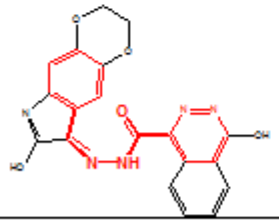			60.6	3.6	25.3	5.6	12.3	0.64
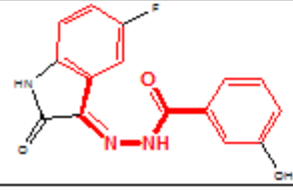			50.0	10.4	10.2	0.4	0.8	0.70

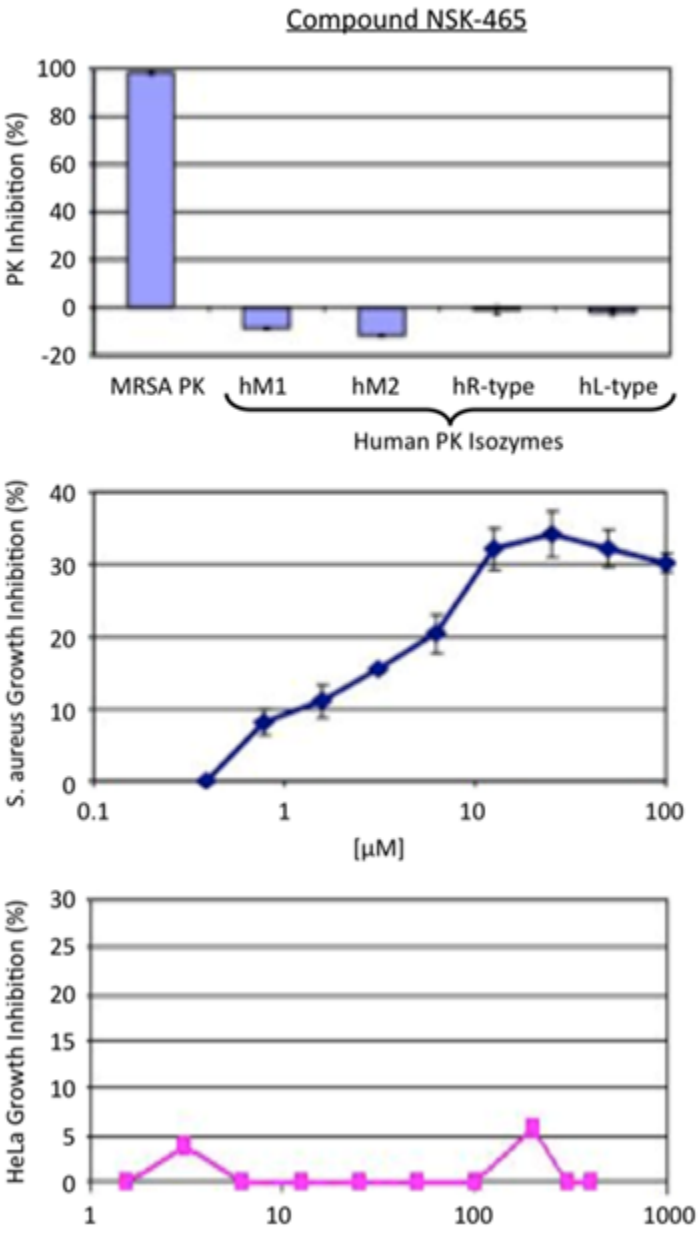

THE UNIVERSITY OF BRITISH COLUMBIA

```
[MRSA PK]   308 VMLSGETAAGLYPEEAVKTMRNIAVSAEAAQDYKKLLSDRTKLVETS--LVNAIGISVAHTALNLNVKA 374
[HUMAN PK]  359 IMLSGETAKGDYPLEAVRMQHLIAREAEAAIYHLQLFEELRRLAPITSDPTEATAVGAVEASFKCCSGA 427
                :******* * ** ***:   : ** .****  : :*:.:  :*.  :    .:* .:.....:::     *
```

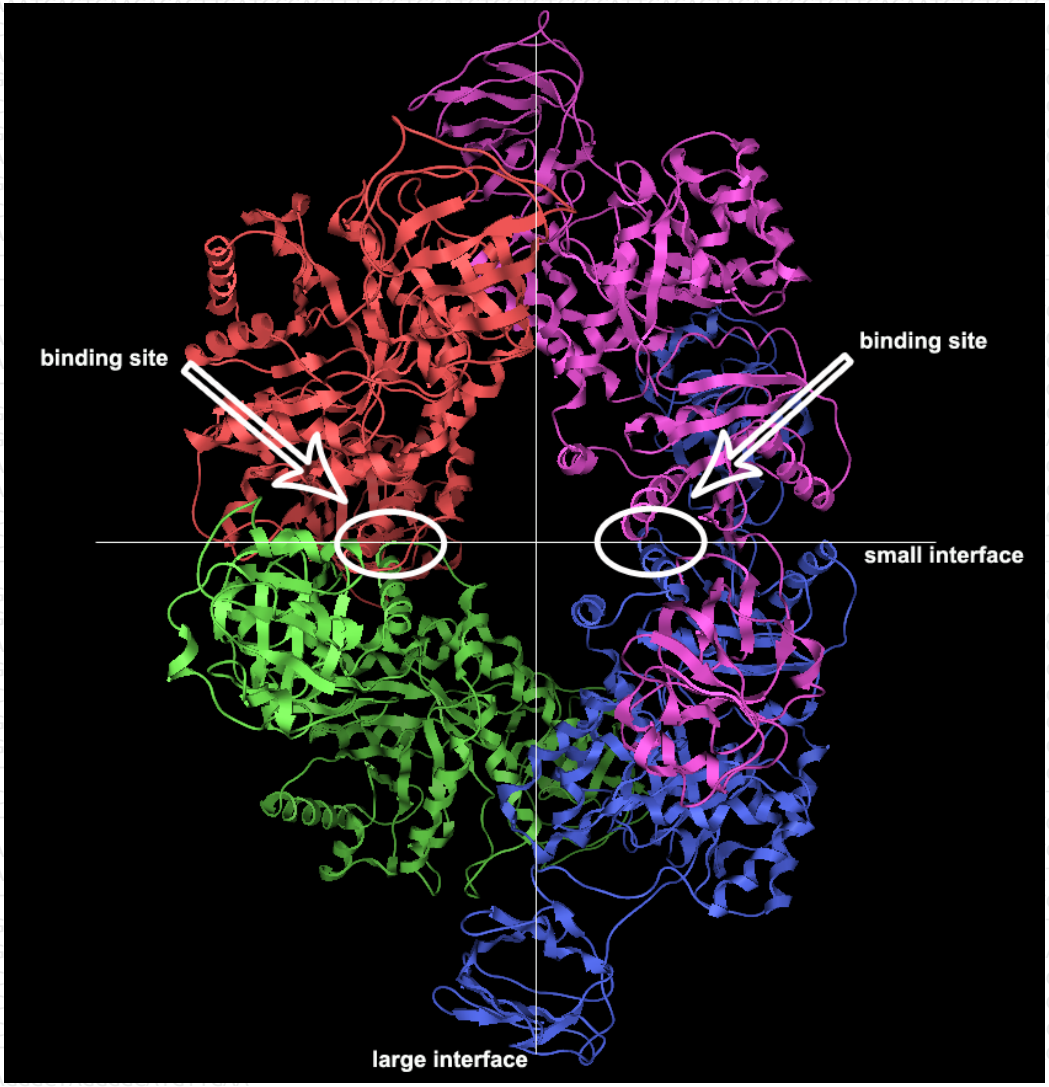

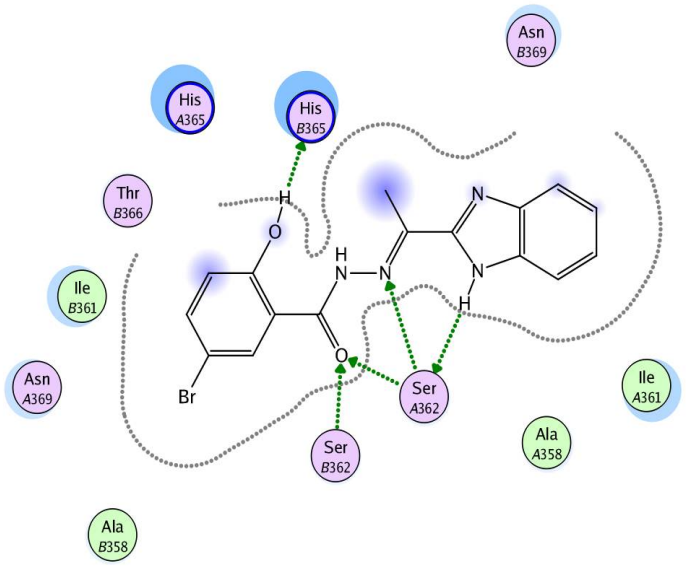

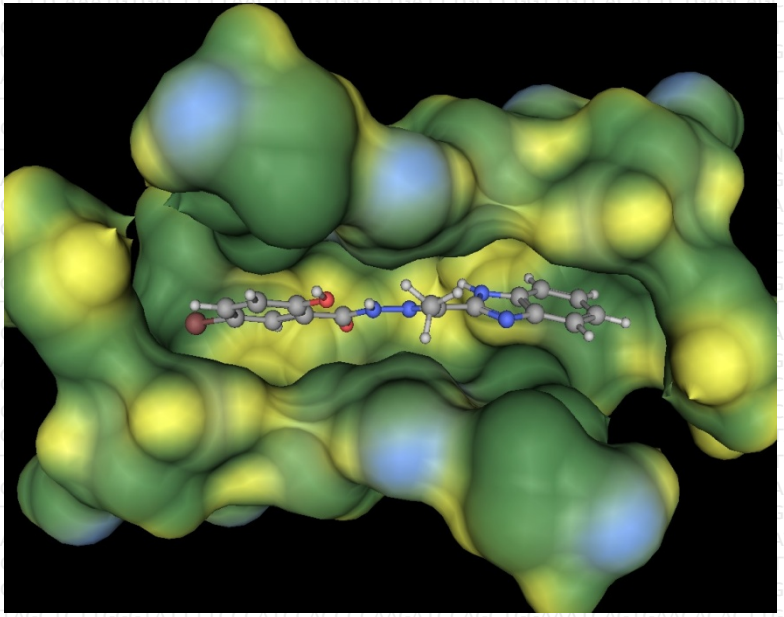

Binding mode of IS-130 at the interface binding site a) A two-dimensional map of the binding interactions between IS-130 and the interface site based on its co-crystallization with MRSA PK. Green arrows depict hydrogen-accepting interactions between IS-130 and MRSA PK residues from the interface. b) Binding orientation of IS-130 within the interface-binding pocket based on the protein-ligand crystallized structure. The protein surface is rendered where green protein surface depicts the hydrophobic interface and yellow depicts the hydrophilic surface.

Synthesis of IS-130 Analogues

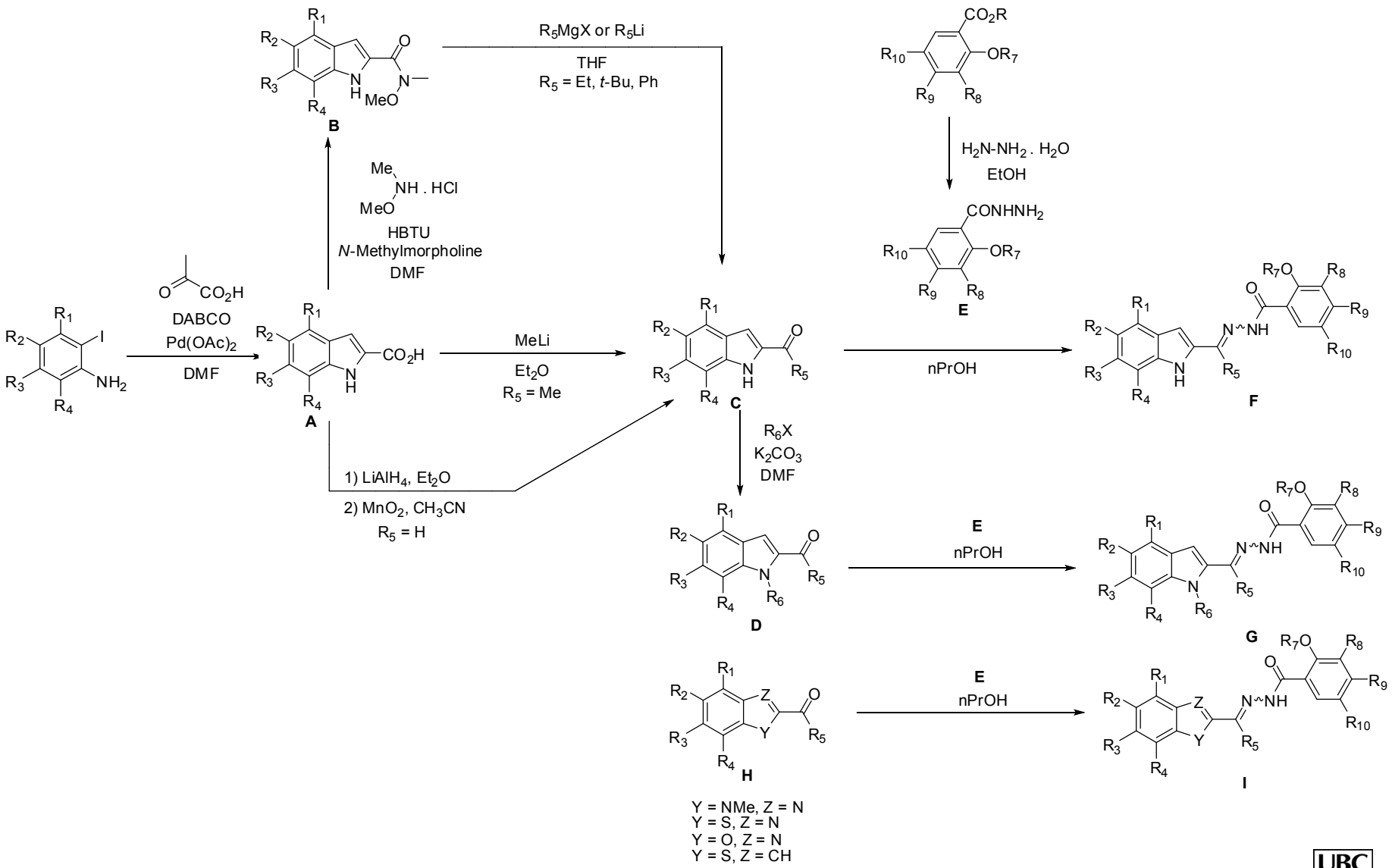

N.S. Kumar et al , 2011

THE UNIVERSITY OF BRITISH COLUMBIA

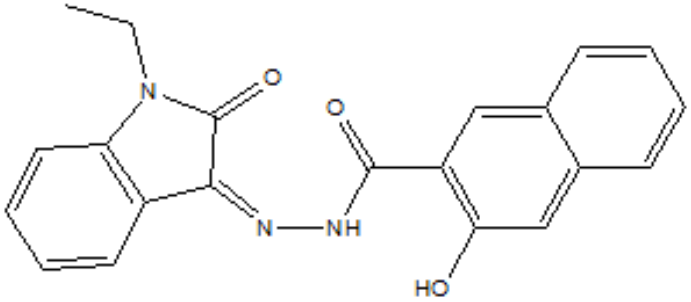

IC_{50} (MRSA Pyruvate kinase) = 911nM

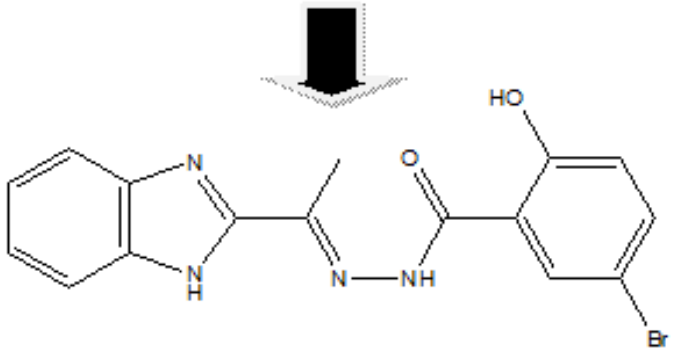

IC_{50} = 91nM

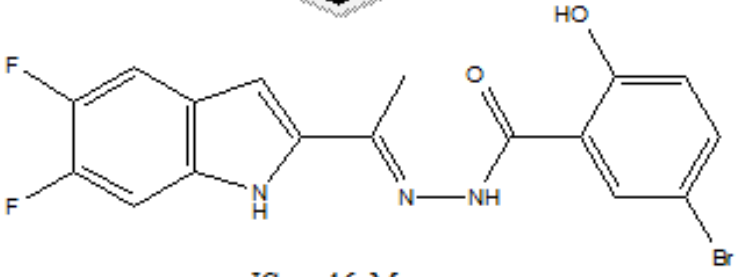

IC_{50} = 16nM

DOCKING

SUBSTRUCTURE SEARCH

MED CHEM OPTIMIZATION

bisIndoles with
IC50 < 1 nM

Table 1
PK inhibitory activity and antimicrobial activity of substituted bis-indoles

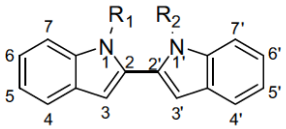

Analogs	IC_{50}[a] (nM)	MIC[b] (μg/ml)	R_1	R_2	Substitutions
10a	21.4	2.0	H	H	6-Bromo
10b	7.0	16.0	H	H	6,6′-Dibromo
10c	2.2	0.3 (3)	H	H	6,5′-Dibromo
10d	2.0	0.3	H	H	6-Bromo-5′-chloro
10e	2.8	0.3	H	H	6-Bromo-5′-fluoro
10f	2.5	>64	H	H	6-Bromo-5′-methoxy
10g	2.2	>64	H	H	6-Bromo-5′-phenyl
10h	36% @ 10 μM	ND	H	H	5-Bromo
10i	3.0	>64 (2)	H	H	5,5′-Dibromo
10j	39% @ 10 μM	ND	H	H	5,6-Dibromo
10k	1.5	0.5	H	H	5,6,6′-Tribromo
10l	2.0	>64	H	H	5,5′,6,6′-Tetrabromo
10m	1.6	1.0	H	H	5,6,5′-Tribromo
12a	1.0	>64 (2)	H	CH_3	6,5′-Dibromo
12b	25% @ 10 μM	ND	CH_3	H	6,5′-Dibromo
12c	1.9	>64	H	CH_2OCH_3	6,5′-Dibromo
14	11.1	>64	H	CH_2COOH	6,5′-Dibromo
15	6.0	>64	H	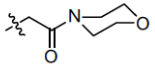	6,5′-Dibromo
17	1.3	2.0	H	CH_2CH_2OH	6,5′-Dibromo
20a	2.0	4.0	H	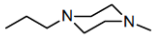	6,5′-Dibromo
20b	1.2	>64	H	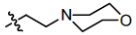	6,5′-Dibromo

[a] IC_{50} values are calculated from a triplicate 15-point titration. Alternatively the % inhibition at the highest concentration tested is presented.
[b] Minimum concentration to give >98% inhibition of growth of *S. aureus* ATCC 29213 (single determination or average of (*n*) determinations). Control MIC (vancomycin) is

Resistance Studies

To assess the potential for cells to become resistance to NSK5-15, we tried to generate resistant mutants by using S. *aureus* RN4220. Cells were passaged for up to 25 consecutive generations in the presence of sublethal concentration of NSK5-15 or for 10 generation with fusidic acid.

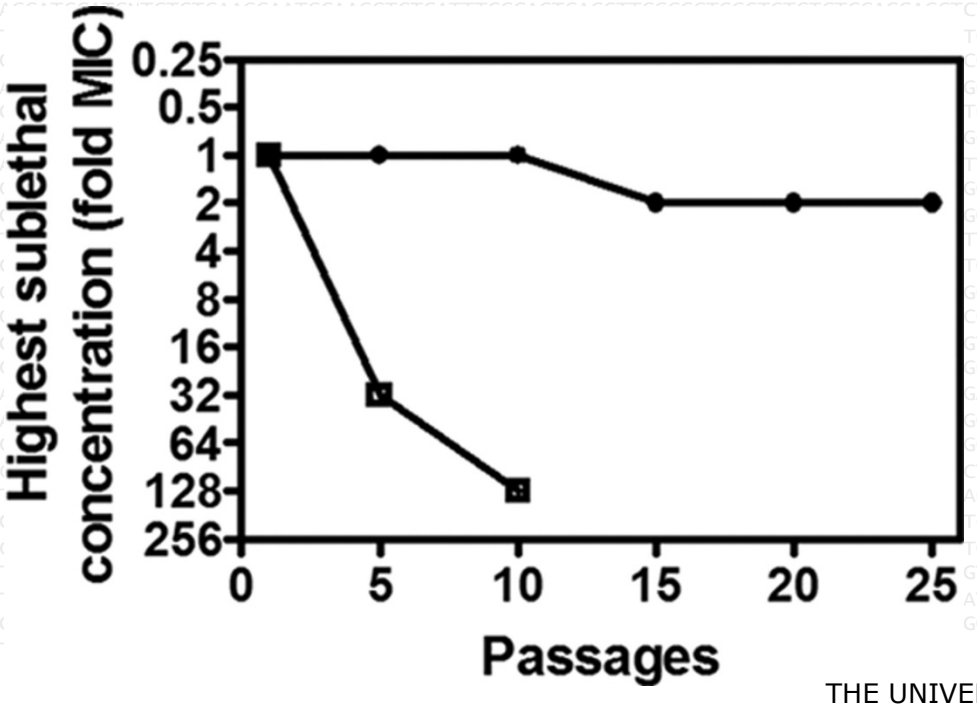

DON’T HUBS ADOPT?

THEY PROBABLY DO… EVENTUALLY

Prostate Cancer

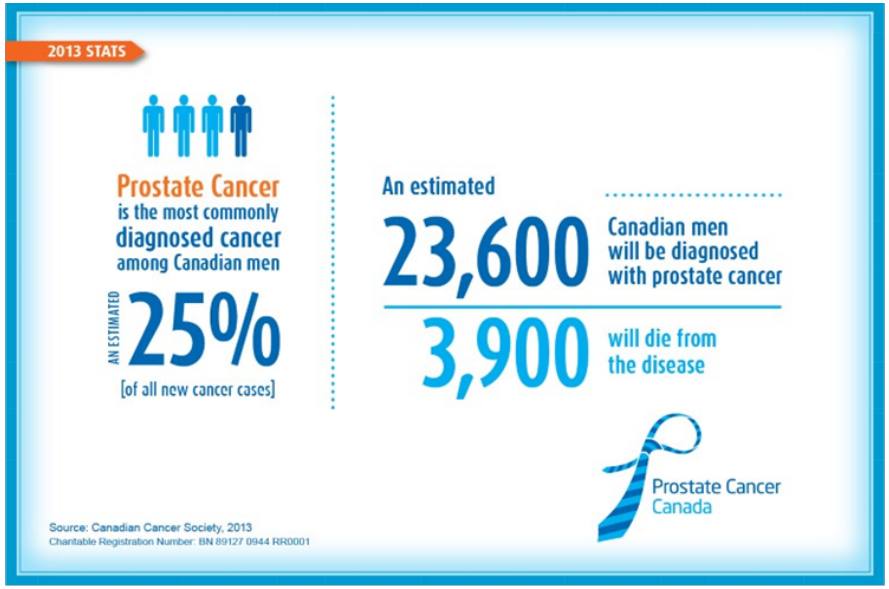

Total estimated cases

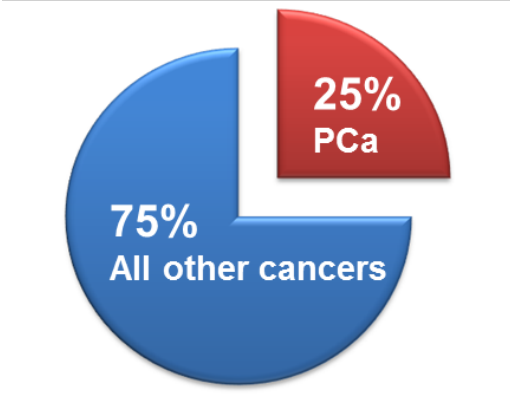

PCa deaths

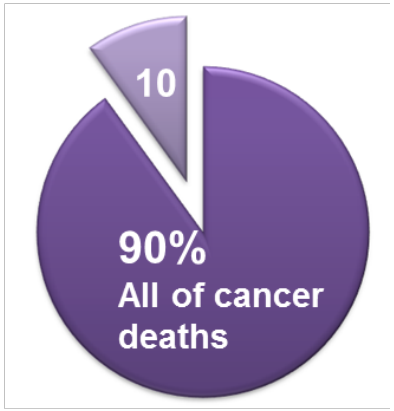

Limitations of Conventional Anti-Androgens

- Mutations in the protein

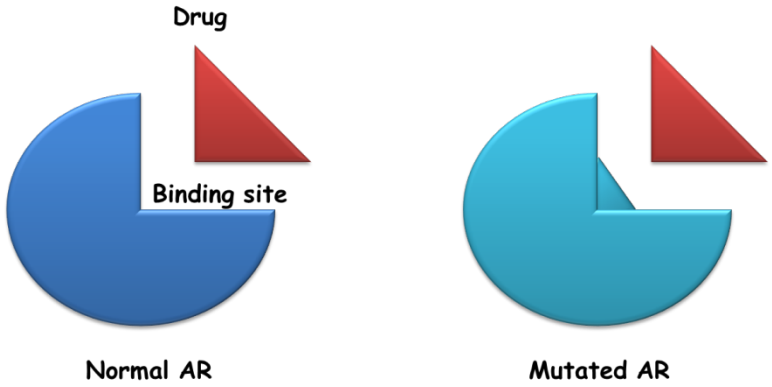

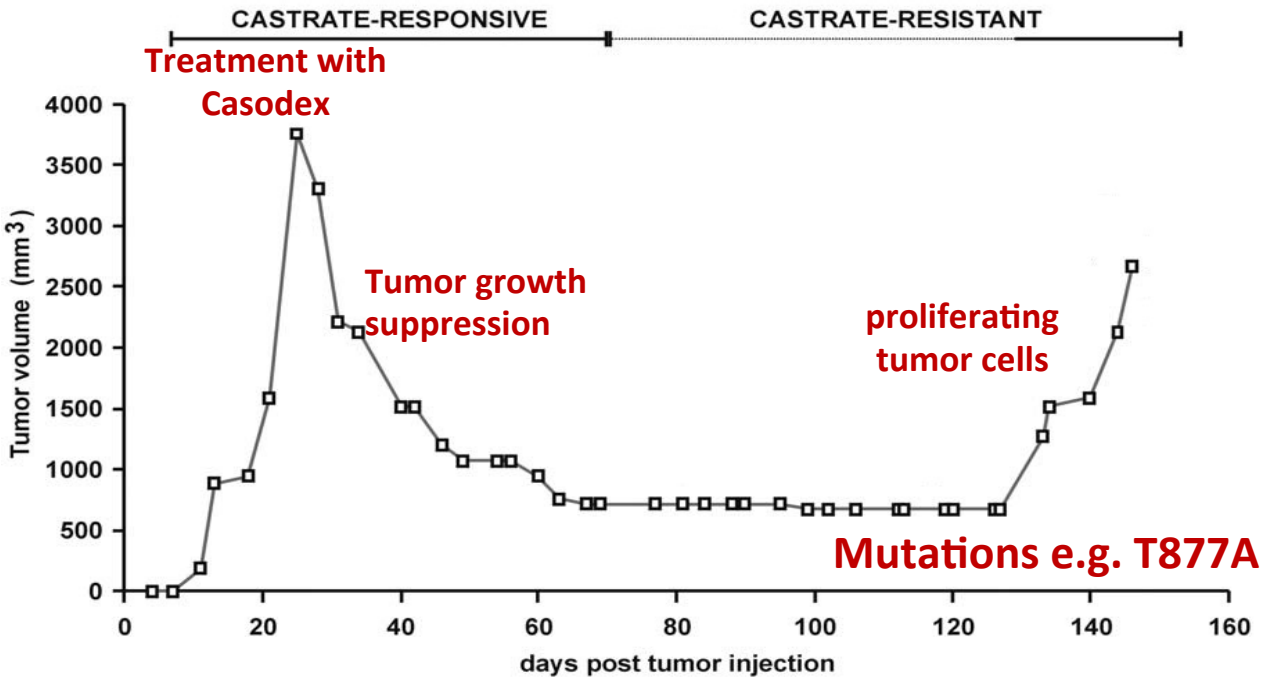

Endocrine-Related Cancer 11 (3) 459 -476

Existing anti-androgens

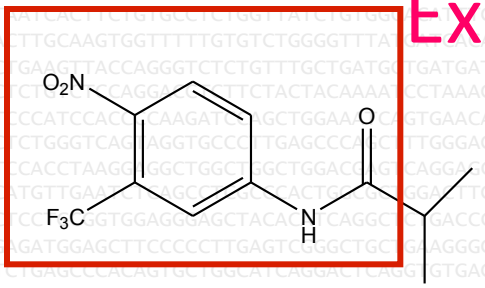

Flutamide

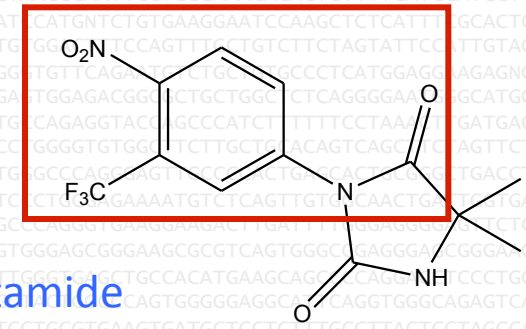

Nilutamide

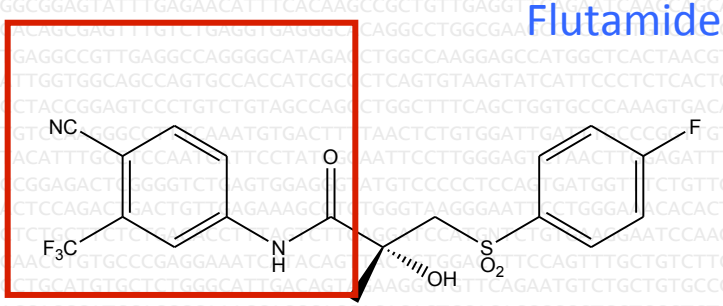

Biglutamide(Casodex)

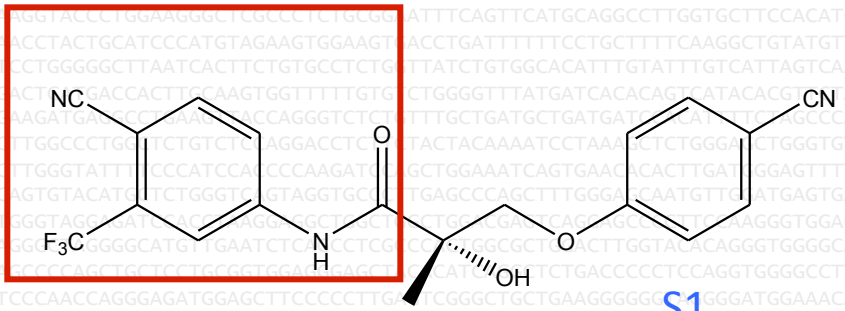

S1

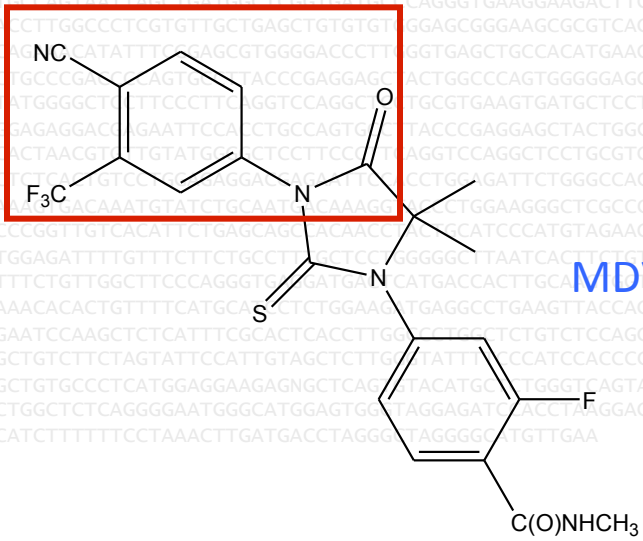

MDV3100 (Enzalutamide)

RU56187

Functional Features of Androgen Receptor

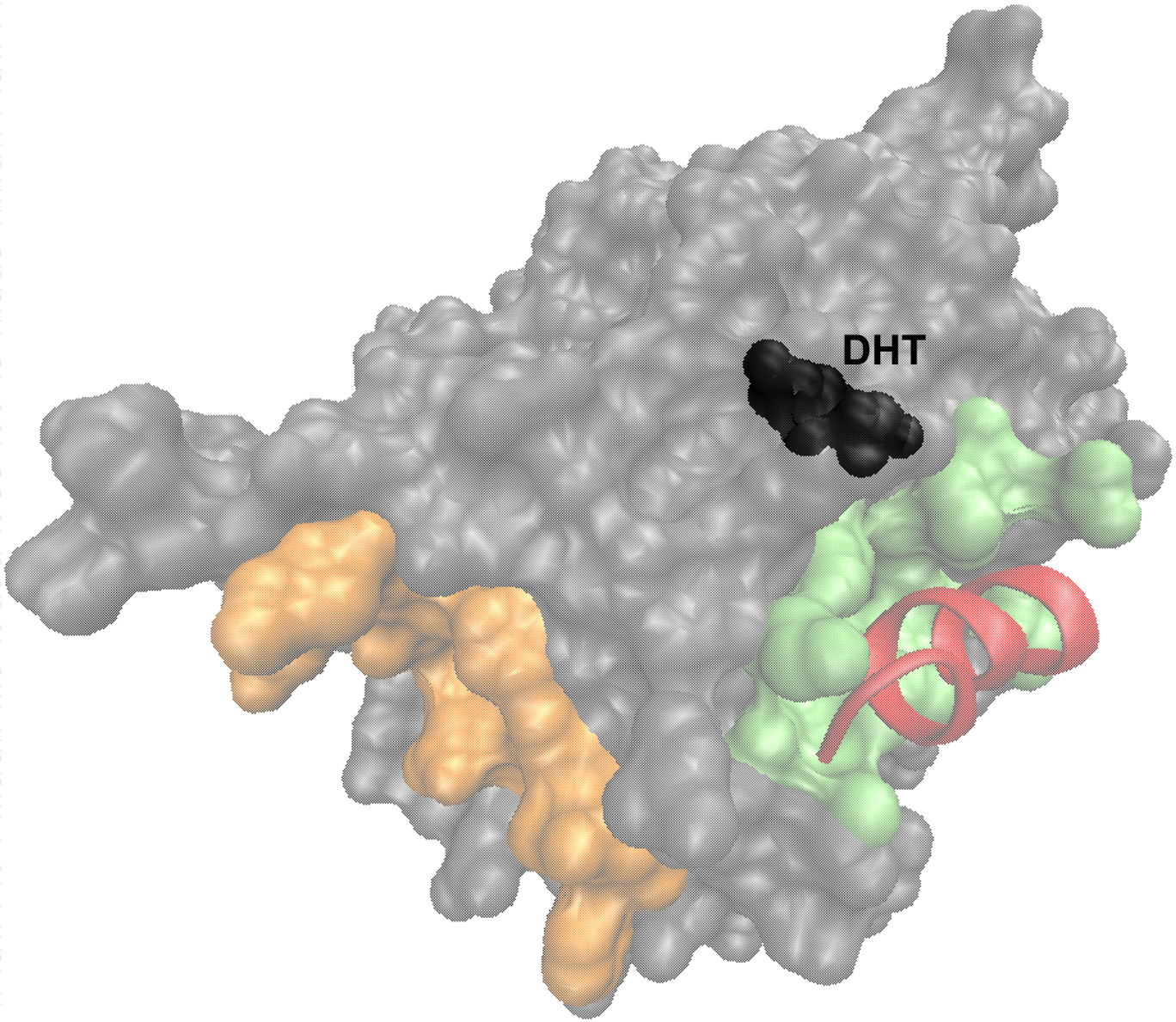

Functional Features of Androgen Receptor

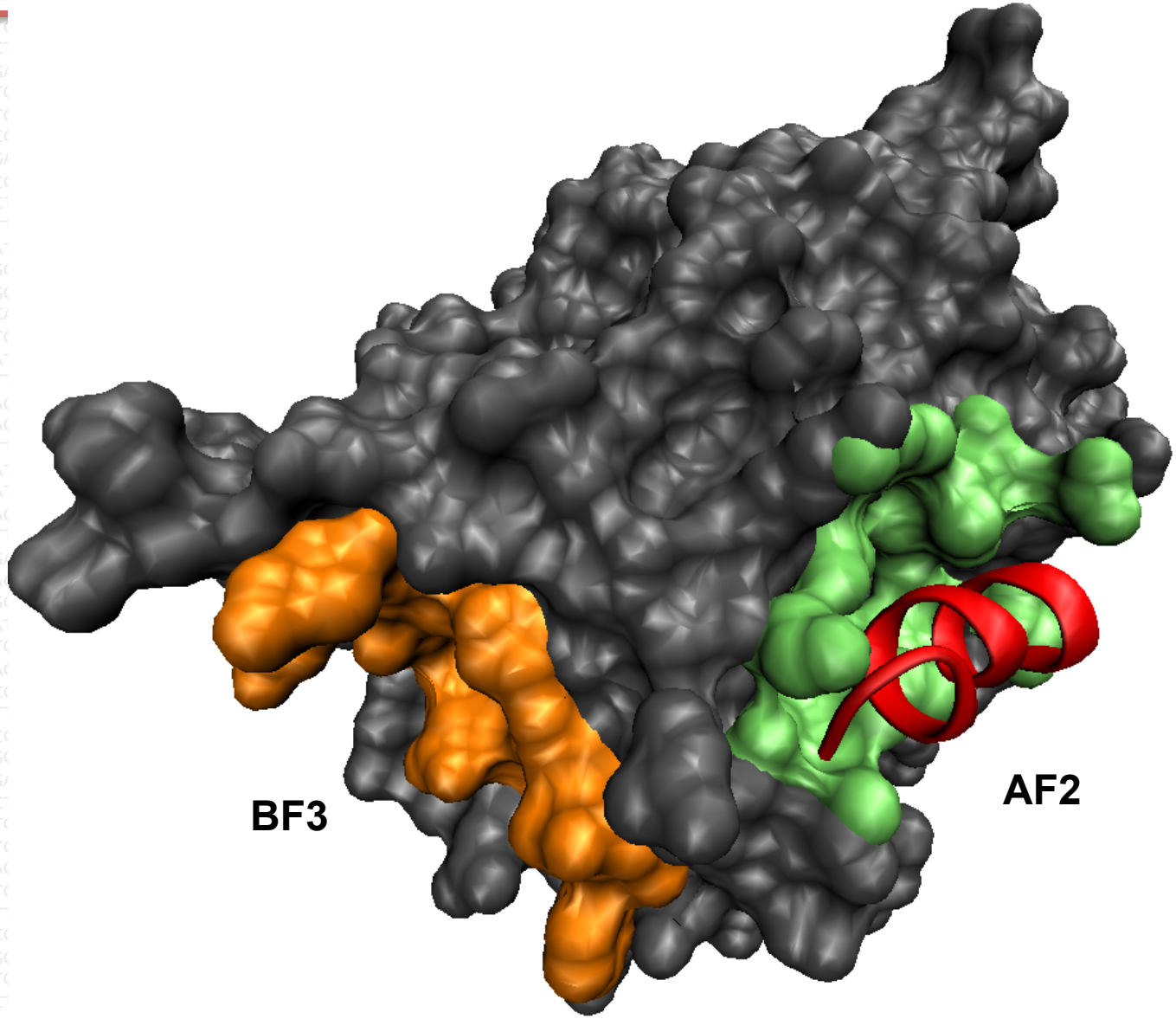

Number of compounds

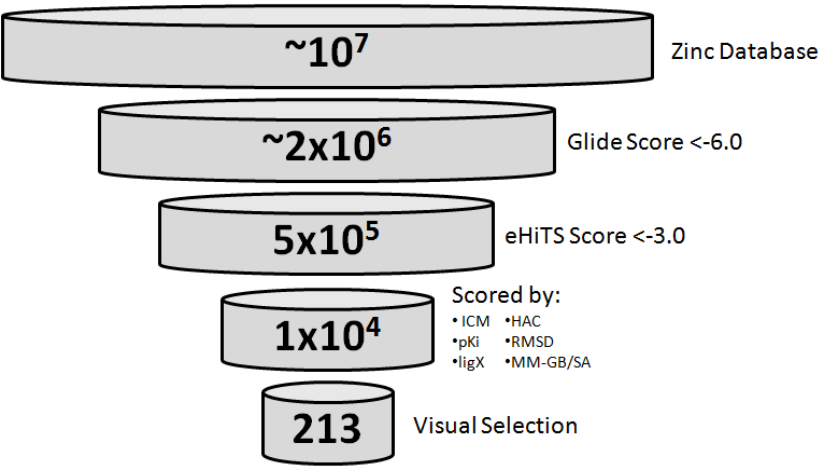

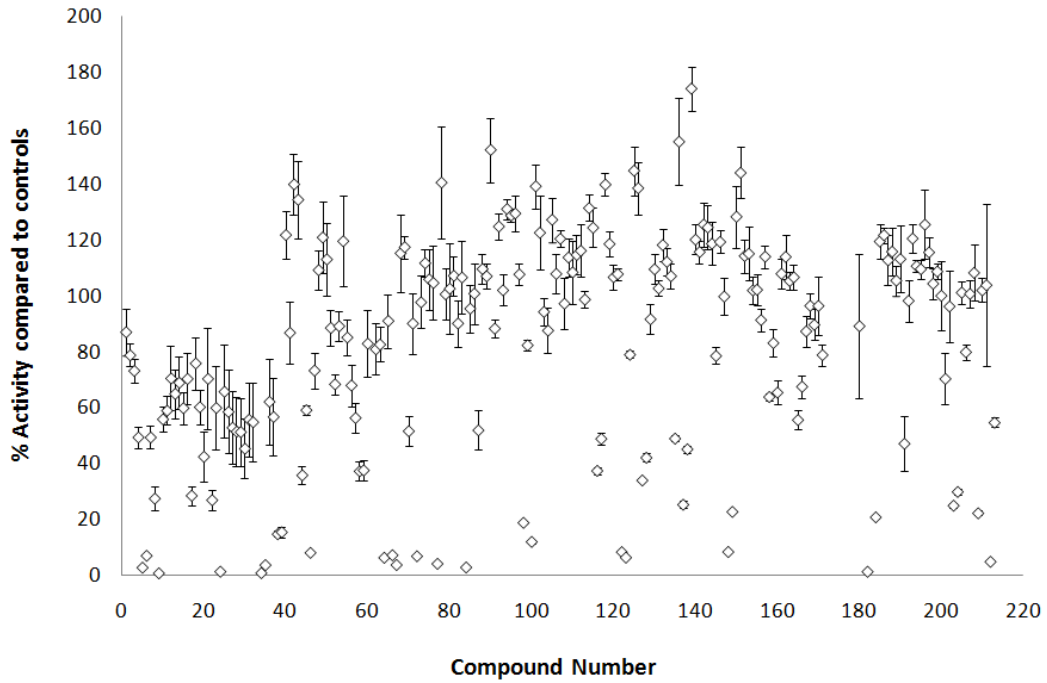

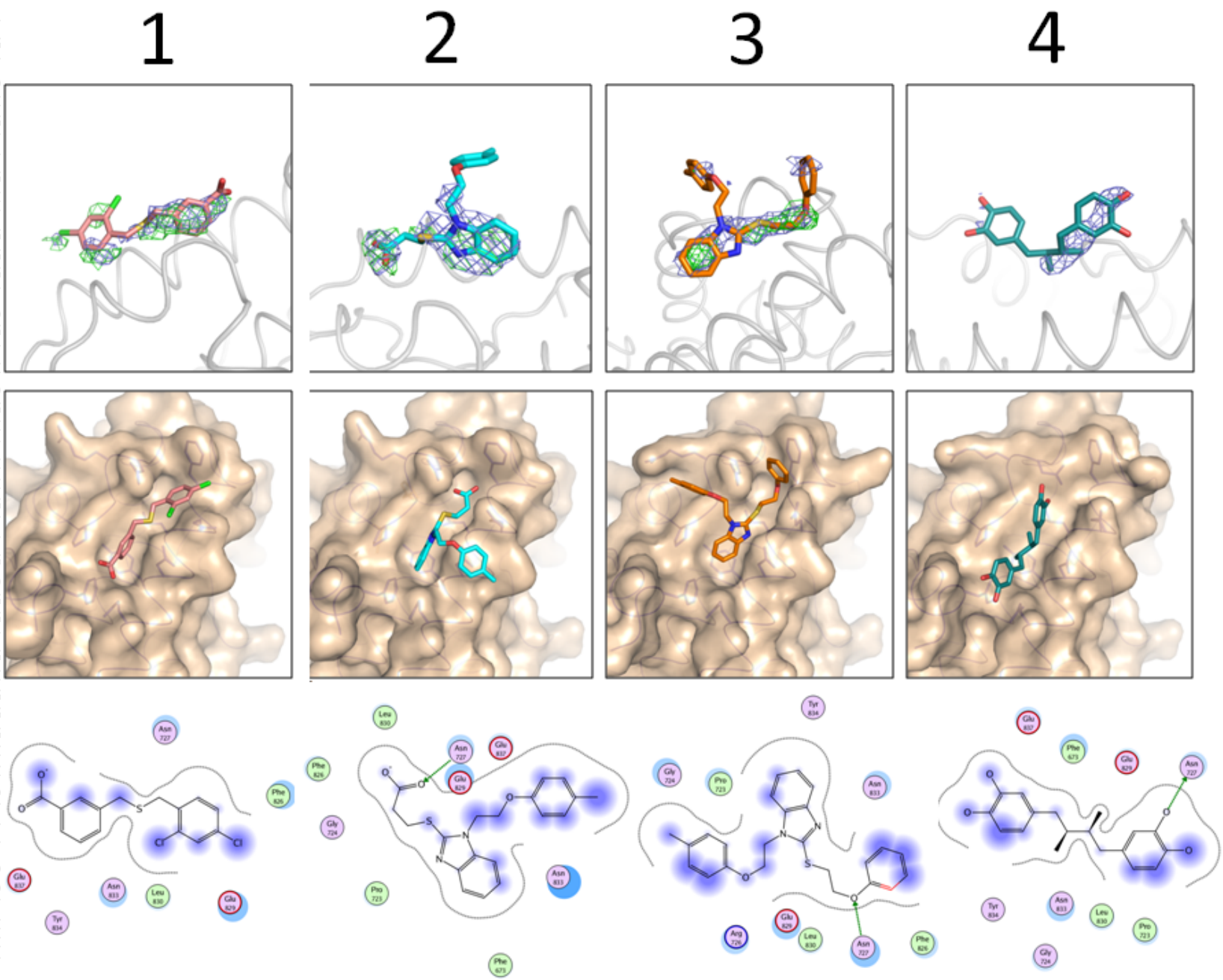
1
2
3
4

Identification of Potent BF3 Inhibitors

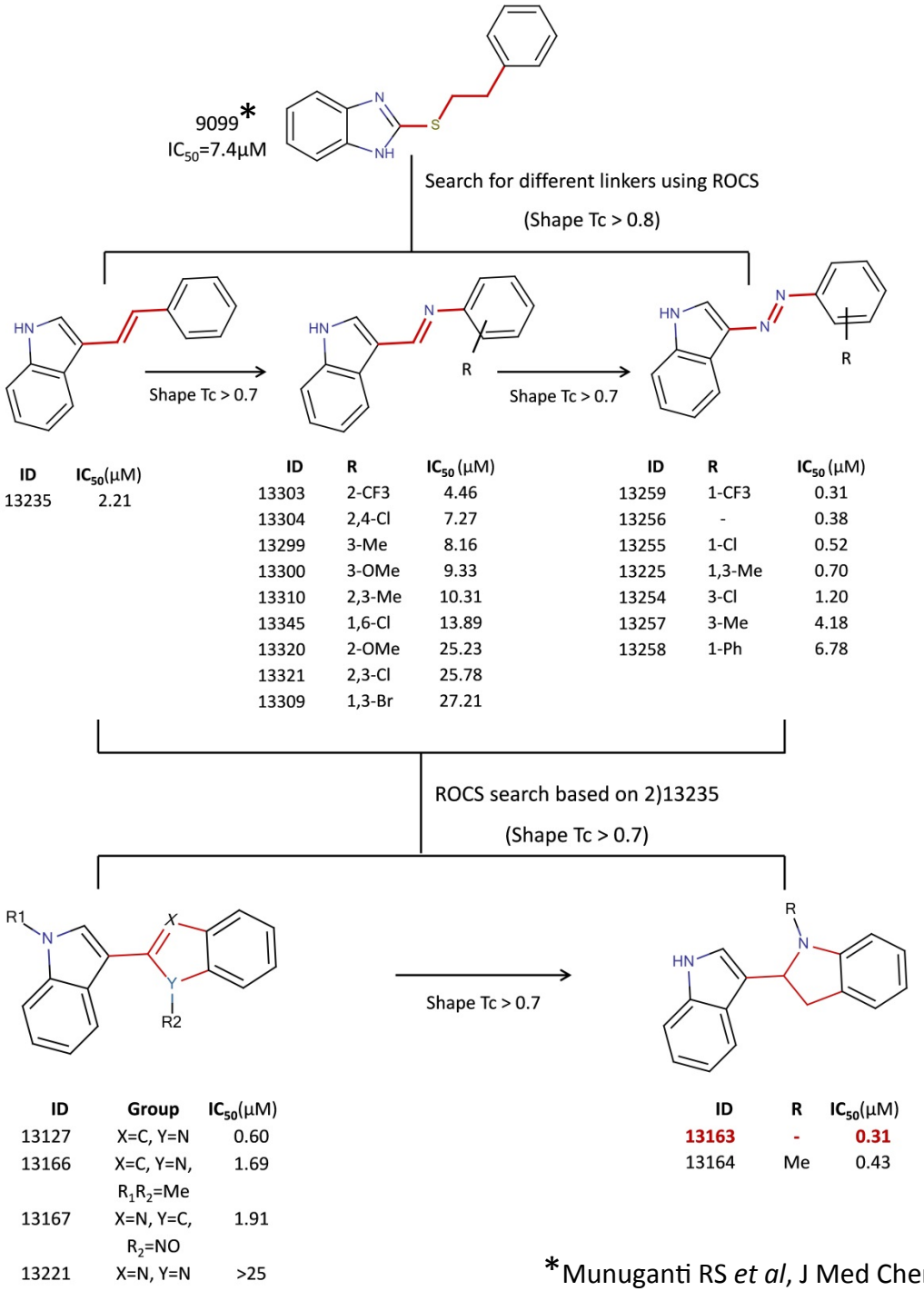

ID	IC_{50}(μM)
13235	2.21

ID	R	IC_{50} (μM)
13303	2-CF3	4.46
13304	2,4-Cl	7.27
13299	3-Me	8.16
13300	3-OMe	9.33
13310	2,3-Me	10.31
13345	1,6-Cl	13.89
13320	2-OMe	25.23
13321	2,3-Cl	25.78
13309	1,3-Br	27.21

ID	R	IC_{50} (μM)
13259	1-CF3	0.31
13256	-	0.38
13255	1-Cl	0.52
13225	1,3-Me	0.70
13254	3-Cl	1.20
13257	3-Me	4.18
13258	1-Ph	6.78

ID	Group	IC_{50}(μM)
13127	X=C, Y=N	0.60
13166	X=C, Y=N, R_1R_2=Me	1.69
13167	X=N, Y=C, R_2=NO	1.91
13221	X=N, Y=N	>25

ID	R	IC_{50}(μM)
13163	**-**	**0.31**
13164	Me	0.43

*Munuganti RS *et al*, J Med Chem, **2013**, 56, 1136

Binding Pose of 13163

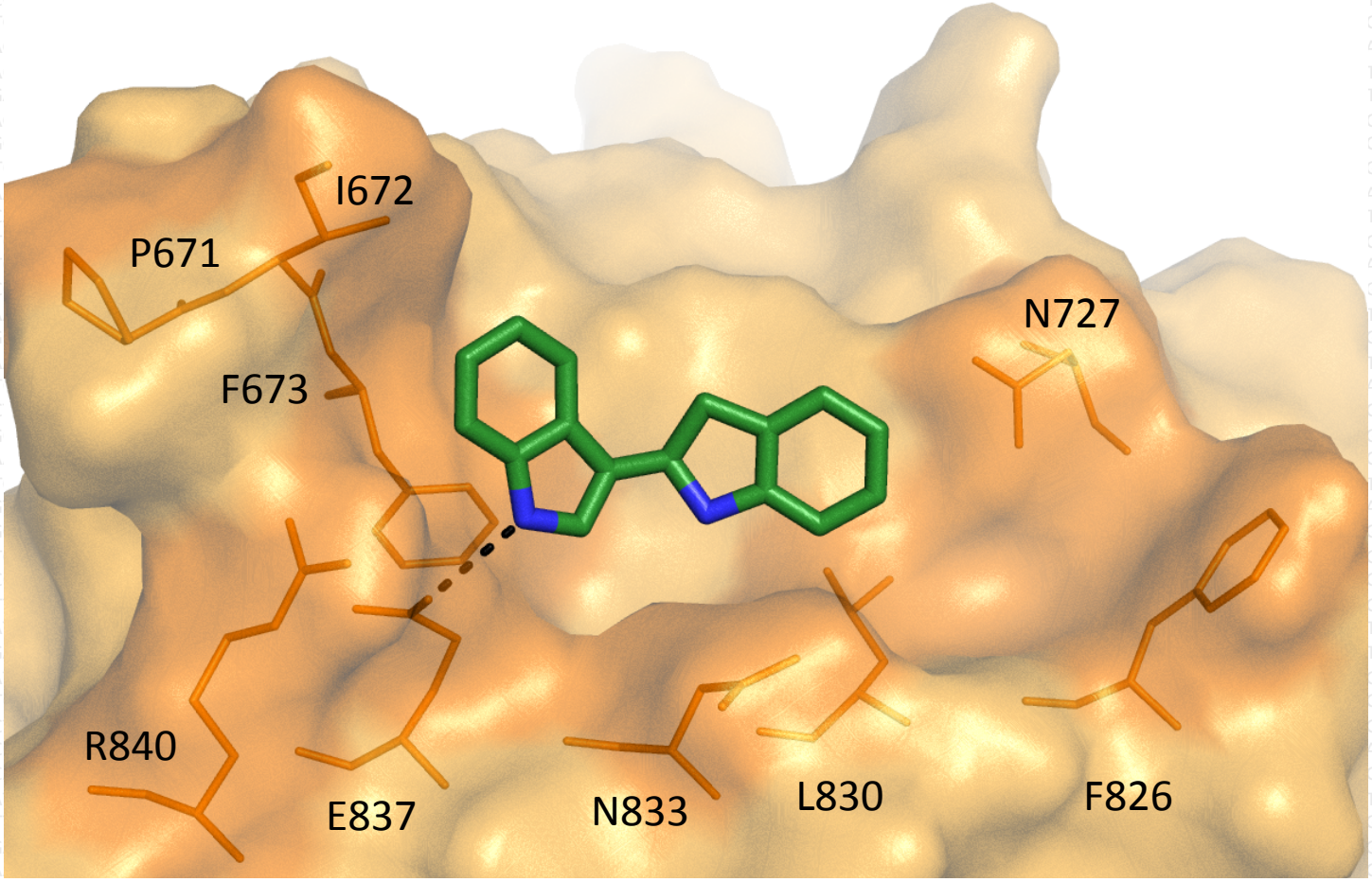

In vitro characterization of 13163

Inhibition of AR translational activity

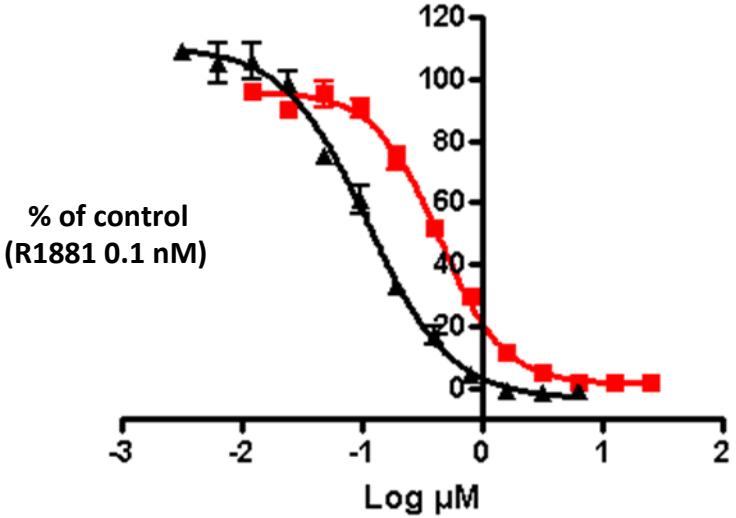

Binding of 13163 to AR LBD

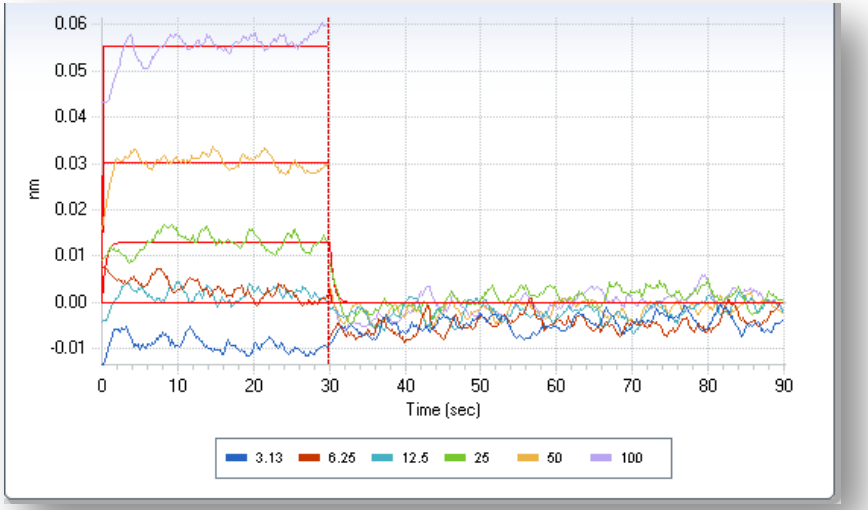

AR eGFP IC_{50}

13163: **0.31 µM**

MDV3100: 0.090 µM

Vpc13163(CMP23 on the chart) and Enzalutamide affect different genes

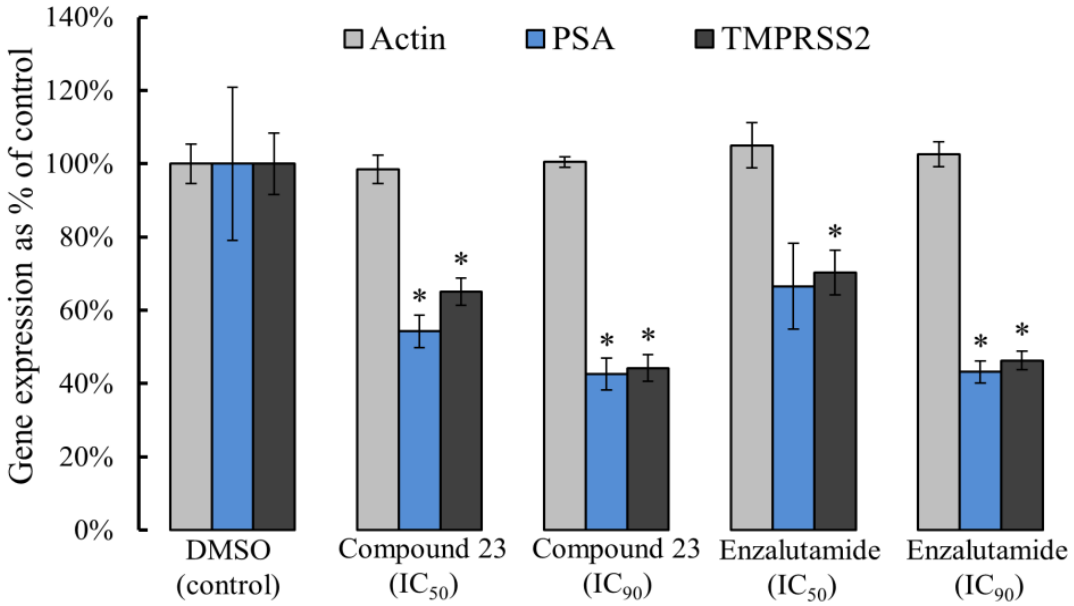

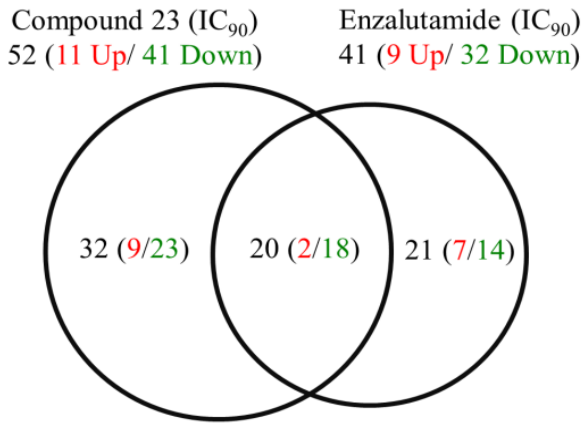

Effect of 13163 on PSA Secretion in LNCaP and Enzalutamide resistant cell line

LNCaP

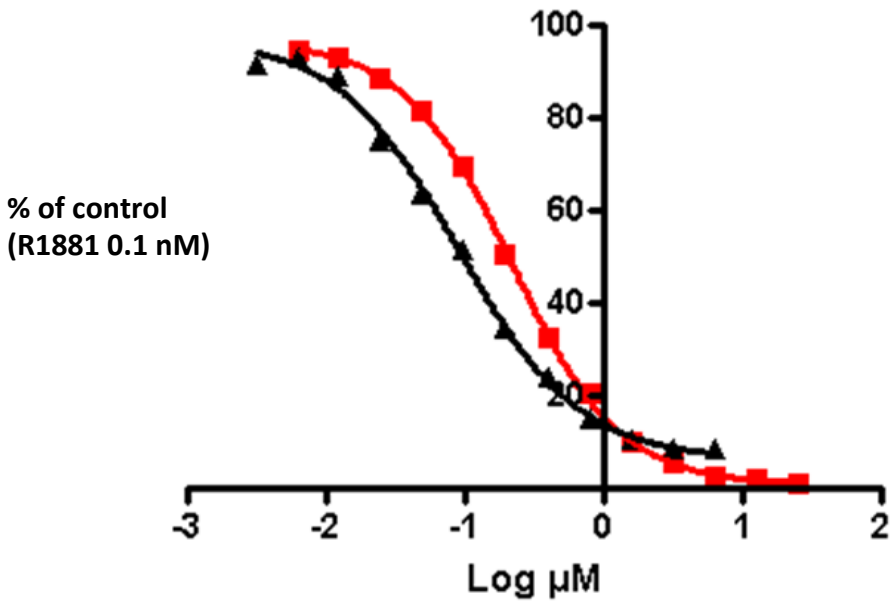

13163: 0.216 µM
Enza: 0.090 µM

MR49F cell line

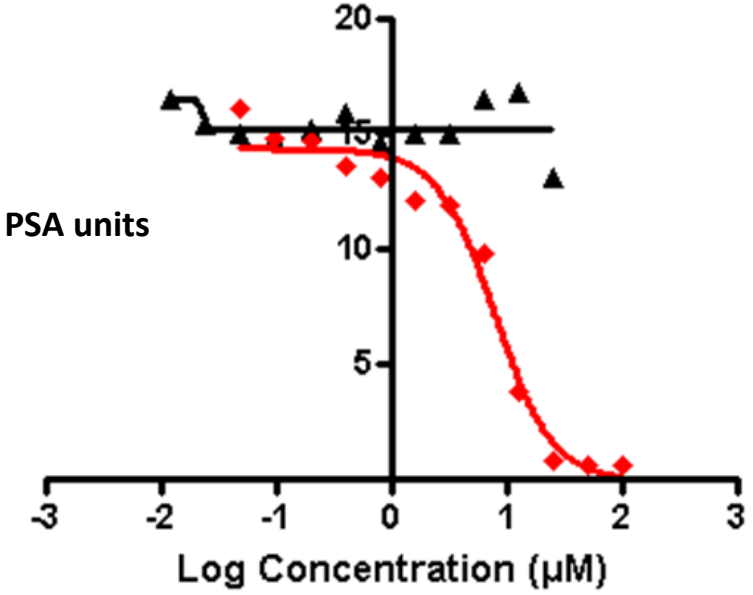

13163: 7.031 µM
Enza: Inactive

Effect of 13163 in Enzalutamide Resistant Mouse Model (tumor volume)

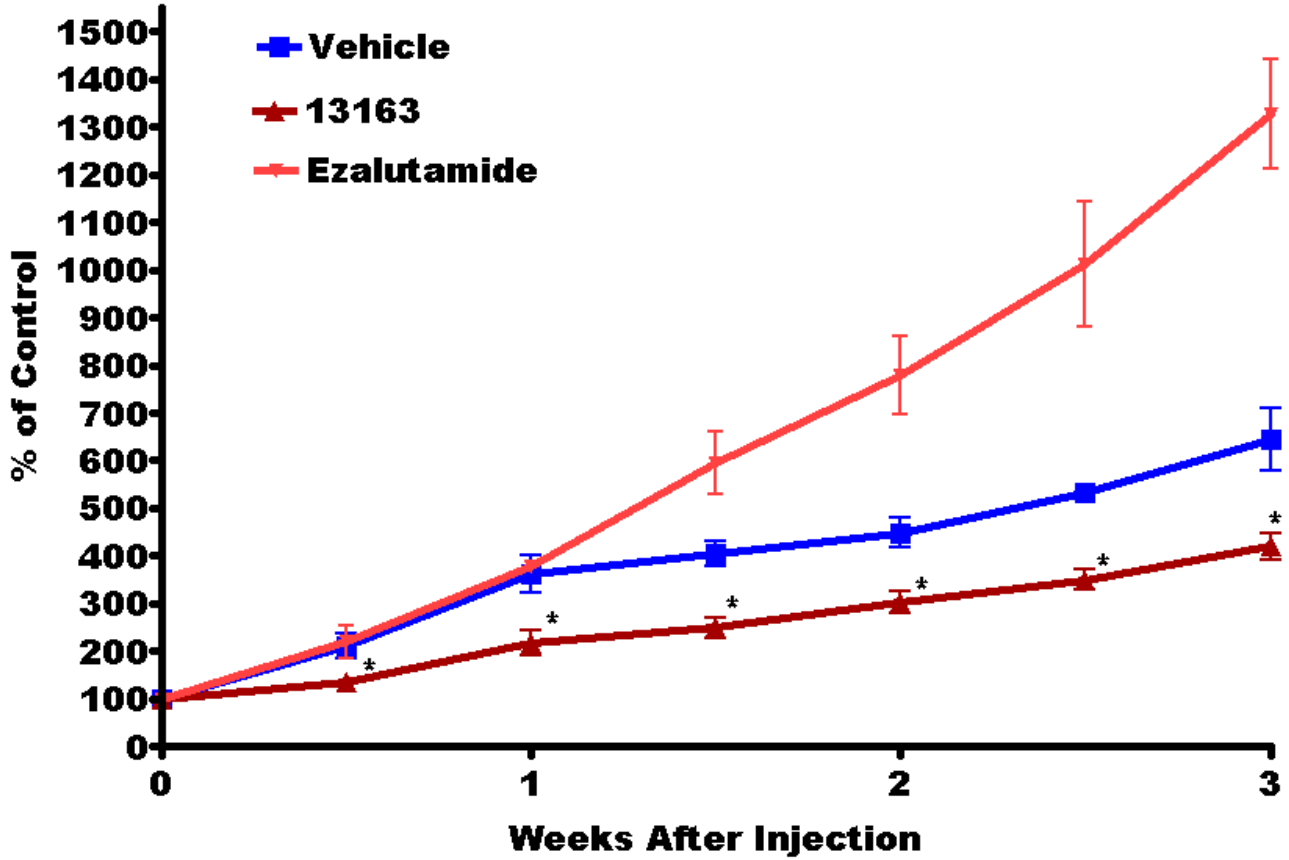

CONCLUSIONS

Hubs PPI represent attractive drug targets,

associated with lower chances of resistance development (example 1)

such PPI inhibitors also help overcoming existing resistance (example 2)

Contributors:

Michael Hsing,
Roya Zoraghi,
Leonard J Foster, Raymond H See,
Nikolay Stoynov, Jihong Jiang, Sukhbir Kaur, Tian Lian, Linda Jackson, Huansheng Gong, Rick Swayze, Emily Amandoron, Farhad Hormozdiari, Phuong Dao, Cenk Sahinalp, Osvaldo Santos-Filho, Peter Axerio-Cilies, Kendall Byler, William R. McMaster, Robert C Brunham, Liam Warrol, Natalie C. Strynadka, Nag S. Kumar, B. Brett Finlay and Neil E Reiner
Emma Guns, Eric Leblanc
Fuqiang Ban, Mohamed Hessein , Ravi Munuganti, Huifang Li
Kate Frewin,Amina Zoubeidi
Robert N. Young (SFU)
Nathan Lack (Koc University)
Robert Fletterick (UCSF)
Martin Gleave
Paul Rennie